

# Fitting a round peg into a round hole: asymptotically correcting the generalized gradient approximation for correlation

Antonio Cancio,<sup>1</sup> Guo P. Chen,<sup>2</sup> Brandon T. Krull,<sup>2</sup> and Kieron Burke<sup>2</sup>

<sup>1</sup>*Department of Physics and Astronomy, Ball State University, Muncie, IN 47306, USA*

<sup>2</sup>*Department of Chemistry, University of California, Irvine, CA 92697, USA*

(Dated: 13 August 2018)

We consider the implications of the Lieb-Simon limit for correlation in density functional theory. In this limit, exemplified by the scaling of neutral atoms to large atomic number, LDA becomes relatively exact, and the leading correction to this limit for correlation has recently been determined for neutral atoms. We use the leading correction to the LDA and the properties of the real-space cutoff of the exchange-correlation hole to design, based upon PBE correlation, an asymptotically-corrected correlation GGA which becomes more accurate per electron for atoms with increasing atomic number. When paired with a similar correction for exchange, this acGGA satisfies more exact conditions than PBE. Combined with the known  $r_s$ -dependence of the gradient expansion for correlation, this correction accurately reproduces correlation energies of closed shell atoms down to Be. We test this acGGA for atoms and molecules, finding consistent improvement over PBE, but also showing that optimal global hybrids of acGGA do not improve upon PBE0, and are similar to meta-GGA values. We discuss the relevance of these results to Jacob’s ladder of non-empirical density functional construction.

PACS numbers: 71.15.Mb 31.15.E- 31.15.ve 31.15.E-,

## I. INTRODUCTION

A major paradigm of the development of density functional theory (DFT) is that of the nonempirical application of constraints within a Jacob’s ladder of approximations. Each rung of Jacob’s ladder<sup>1</sup> is characterized by its treatment of the exchange-correlation (XC) energy, the only component of the total energy approximated within the Kohn-Sham scheme. The rungs are to be filled with approximations that satisfy relevant exact constraints. An optimal functional at a given rung should presumably incorporate the maximum amount of information that a functional of that form can.<sup>2</sup> Each approximation should improve over that of lower rungs, usually at higher computational cost.

The ground-level is the Hartree approximation (i.e., XC set to zero); the first rung is the local density approximation (LDA), whose form is unambiguously determined by the XC energy of a uniform electron gas. The local gradient of the density is added at the next rung, the generalized gradient approximation (GGA). For the last two decades, the PBE functional<sup>3</sup> has been a popular candidate for this level.<sup>4</sup> Its moderate accuracy for a very broad range of systems is because it agrees in large part with the real-space cutoff (RSC) construction for a GGA,<sup>5,6</sup> and in so doing, satisfies seven exact constraints.<sup>3</sup> The third or meta-GGA rung adds the kinetic energy density<sup>7</sup>, or alternately, the Laplacian of the density.<sup>8–12</sup> This rung has been much harder to fill nonempirically, but recently, the SCAN functional,<sup>2</sup> constructed with a combination of exact conditions and appropriate norms, promises to become a new standard, overcoming difficulties of previous attempts.<sup>13–18</sup> By the logic of Jacob’s ladder, SCAN should outperform the LDA and

non-empirical GGAs like PBE in almost all areas.

A problem with the nonempirical approach is that of finding effective constraints to optimize a given level of functional. Finding the optimal constraints to use at a given level is an ill-posed problem – often the satisfaction of a constraint with a lower-rung form requires breaking other, perhaps equally important constraints. Thus many alternatives to PBE have been developed by choosing alternative sets of constraints.<sup>19–27</sup> At the meta-GGA level, the flexibility of the form allows many more constraints to be satisfied, but the problem then is the sheer complexity of the form required to do so, and finding enough relevant constraints to constrain it. For the GGA level, because the gradient expansion of the real-space hole is known for both X and C, a GGA can be numerically defined by cutting off that hole in real-space. The exact conditions met by the resulting RSC GGA are largely those that are implemented in the construction of the PBE.

In this context, the concept of “appropriate norms” as described in Ref. 2 takes on importance. These are paradigmatic systems that a density functional at a given level of approximation rigorously satisfies. The importance of norms are that they contain more information than other forms of constraints, and eliminate much of the ambiguity involved in their application. The fundamental example is the homogeneous electron gas that exactly specifies the LDA. Unfortunately no such unambiguous norms exist for the GGA level or meta-GGA level, although the removal of correlation self-interaction in single-electron systems, a limited norm, is a key target of non-empirical meta-GGAs.

Indeed, the absence of such a norm for a GGA guided the original development of constraint-based GGA func-

tionals in terms of the numerical RSC model for the exchange-correlation hole (which describes XC-induced fluctuations in electron density about any electron.) GGAs capture some general features of this hole, but lack the capacity to describe the hole of any real system in detail – in a sense similar to fitting a round peg into a square hole. This limitation underlies the ambiguity in the formulation of nonempirical GGAs.

Over the last decade<sup>28–32</sup> the semiclassical analysis of the electron gas has identified what might be considered the most significant norm for DFT. An especially fruitful aspect of this approach is the analysis of the limit in which the external potential and number of electrons are simultaneously scaled to infinity.<sup>29,33–35</sup> This scaling is familiarly manifested by the extension of the periodic table of neutral atoms to the limit  $N = Z \rightarrow \infty$ . Semiclassical analysis<sup>30–32,36–41</sup> derives the LDA as the natural limit of this process for any system and generates an expansion in inverse nuclear charge that then yields universal corrections to the LDA that may be satisfied by semilocal GGAs, thus in principle generating the first two rungs of Jacobs ladder. In turn, the fourth-order gradient correction, frequently used in constructing meta-GGA’s, along with higher gradient corrections is expected to make a contribution only to higher orders in the large- $Z$  expansion.<sup>26,30</sup> While in simple, one-dimensional non-interacting systems such corrections can be explicitly derived<sup>42,43</sup>, for real systems, such corrections can at present only be extracted numerically, and so far, only for atoms and similar simple cases.

Recent work has provided numerical estimates of these corrections for the exchange energy and Kohn-Sham kinetic energy.<sup>30,31</sup> Correlation has awaited the availability of highly accurate total correlation energies for a significant subset of the atoms via quantum chemical methods.<sup>44,45</sup> Recent work<sup>32</sup> has used this data to identify precisely the leading energetic correction to LDA for the correlation energy of neutral atoms. This correlation constant is likely correct at least for non-periodic Coulombic systems, and perhaps universally, and we can numerically extract its value for neutral atoms, and hence build it into approximate functionals. This is entirely non-empirical, and in principle, its value could be determined by a long perturbative semiclassical calculation, as has been done previously at the LDA level for correlation. A similar (but much simpler) derivation for exchange showed that both the B88 and PBE exchange functionals come quite close to fulfilling the equivalent exact condition for exchange.<sup>31</sup>

This new information offers a potential resolution to the issue of finding an appropriate norm for the GGA. Just as the LDA forms the leading order term in the asymptotic expansion of correlation (indeed of any component of the energy) the GGA is the simplest possible functional which can reproduce the leading order beyond-LDA term in the expansion, that is, the order characterized by our recent extrapolations. Moreover, the process of estimating the high- $Z$  correction to the LDA from low-

$Z$  data involves constructing a smooth asymptotic form that approximates the semiclassical asymptotic expansion for correlation to all orders of  $Z$ . This smooth form, accurately reproducing quantum chemistry (QC) data for all  $Z$ , is in principle exactly fit by a GGA, as we shall show in the course of this paper. Higher rungs of Jacobs ladder appear as corrections to this smooth form, and generate, for atoms, rich and complex shell structure effects beyond the scope of this paper. We argue then that the high- $Z$  limits of atomic exchange and correlation energies and the related approximate smooth asymptotic forms for all  $Z$  define an appropriate norm for the construction of the GGA. That is, asymptotic analysis produces the “round hole” that the “round peg” of the GGA can (and should) be made to fit.

The purpose of this work then is to construct a GGA-level functional that is asymptotically correct – exact in the large- $Z$  limit of neutral atoms. A notable parallel in behavior<sup>32</sup> between PBE correlation and the smooth asymptotic trend of QC correlation data makes PBE the natural reference for constructing an asymptotically correct functional. In the present work, however, we show that in the semiclassical limit there is a significant contribution to the correlation GGA that is *undetermined* in the PBE derivation, defining a new, eighth constraint, that a nonempirical GGA should satisfy rigorously. By modifying the high density limit of PBE correlation (PBEc), we enforce this new exact condition on GGA, and agree better with the high density limit of the real-space cutoff procedure. This variation on PBE, which we call acGGA (asymptotically-corrected GGA) has vanishing relative error in the non-relativistic limit of large  $Z$ , and results show that acGGA yields the most accurate GGA for atomic correlation energies in this limit. We also develop a corresponding modification to PBE exchange, and find strong cancellation of errors between X and C for the atoms in acGGA. The end result is a significant improvement over PBE for all atoms with  $Z > 1$ . We test this acGGA for a small set of molecular atomization energies, showing a moderate and consistent improvement over PBE, showing that for main-group small-atom molecules, acGGA improves upon PBE performance.

For real systems, relativistic effects grow with  $Z$  and become indispensable around  $Z = 50$  (the precise ground-state configuration of even Ni depends on them), but this is beside the point for the present study. The available norms, numerical correlation energies for the homogeneous electron gas and spherical atoms, are specifically derived for the nonrelativistic case. More to the point, the main lesson of semiclassical analysis is that the  $Z \rightarrow \infty$  limit has much to say about finite  $Z$  atoms, including low  $Z$  where relativistic effects are not important.

We also note numerous attempts to improve exchange at the generalized gradient approximation level from constraint-based considerations<sup>3,19–22,24,25</sup> but rather fewer forms<sup>3,19,46,47</sup> for correlation, most notably the early PW91<sup>19</sup> and PBE functionals. This paper answers

why this should be the case in terms of the different asymptotic behavior of exchange and correlation, and particularly the asymptotic behavior of PBE correlation and its relation to the real-space cutoff model of the correlation hole.

It is unlikely that acGGA will replace PBE in actual practice; nevertheless it is vital that each rung of Jacob's ladder incorporate the relevant exact conditions and norms for that rung. Here we implement an insight as to what the correct GGA rung should look like. Having each rung correct is vital for studying the corrections to be included at the next level. The SCAN functional is unlikely to be the last word in meta-GGAs, but it includes these asymptotic constraints, in a form different from that developed here.<sup>2</sup> We also note a preliminary report concerning asymptotically correcting the GGA.<sup>48</sup>

This paper is organized as follows. In Sec. II we discuss the theoretical background of our work: reviewing the asymptotic analysis of the energies of atoms and Lieb-Simon scaling, recent findings for correlation, the RSC procedure and how it is used to construct PBE. Sec. III describes the construction of an asymptotically corrected GGA. In Sec. IV, we test our functional against correlation energies for the periodic table of atoms and heats of formation of molecules, discussing successes (GGA) and limitations (hybrid). Sec. V discusses implications for future density functional development, and for understanding the asymptotic limit of atoms, followed by conclusions.

## II. THEORY OF ASYMPTOTIC EXPANSION

### A. The Lieb-Simon limit

In a landmark 1973 paper, Lieb and Simon proved rigorously that simple Thomas-Fermi (TF) theory,<sup>33</sup> the precursor to modern Kohn-Sham DFT, becomes relatively exact in a very specific limit, which can be treated with semiclassical approximations. In this subsection, we show how that limit can be approached for any electronic problem, how the various components of the energy behave in this limit, and how the dominant contributions in GGA correlation are determined by this limit.

#### 1. Lieb-Simon scaling

Lieb-Simon  $\zeta$ -scaling<sup>29,34,35</sup> captures a fundamental pattern of the periodic table in a continuous scaling relationship, relating this fundamental intuitive tool of chemistry to a formal mathematical framework. It is defined as follows: for a system of  $N$  non-relativistic electrons and a one-body potential  $v(\mathbf{r})$ , the  $\zeta$ -scaled system may be defined as

$$v_\zeta(\mathbf{r}) = \zeta^{4/3} v(\zeta^{1/3}\mathbf{r}), \quad N_\zeta = \zeta N, \quad (1)$$

where  $1 \leq \zeta < \infty$ . This amounts to scaling the coordinates of the system while simultaneously increasing the number of particles. Taking the potential

$$v(\mathbf{r}) = -1/r, \quad v_\zeta(\mathbf{r}) = -\zeta/r, \quad (2)$$

and setting  $N = 1$  corresponds to mapping the Hamiltonian of a neutral hydrogen atom to a neutral atom of nuclear charge  $Z = \zeta$ . Note that in this case,  $\zeta$  is a continuous generalization of  $Z$ .

Crucially for our work, Lieb and Simon show<sup>33,34</sup> that the Thomas-Fermi energy is the rigorous limit of the electronic energy – as  $\zeta \rightarrow \infty$ ,

$$\lim_{\zeta \rightarrow \infty} \frac{E(\zeta) - E^{\text{TF}}(\zeta)}{E(\zeta)} \rightarrow 0. \quad (3)$$

This holds for nuclear potentials and more generally a large class of external potentials that have bound states.<sup>49</sup>

Thus  $\zeta$ -scaling extracts the simplest possible density functional theory, Thomas-Fermi theory, from any starting point, however complex.<sup>50</sup> Note that this process does not produce a simple coordinate scaling of the ground-state charge density. For example, transforming one atom into another necessarily generates differences in shell structure. However, as  $\zeta \rightarrow \infty$ , this shell structure becomes vanishingly small and the density  $n_\zeta$  of the scaled system tends to the Thomas-Fermi limit:

$$n_\zeta(\mathbf{r}) \rightarrow n_\zeta^{\text{TF}}(\mathbf{r}) = \zeta^2 n^{\text{TF}}(\zeta^{1/3}\mathbf{r}). \quad (4)$$

Here  $n^{\text{TF}}(x)$  is a smooth, universal scaling form, normalized to one. It does not have a simple closed form, but has been recently accurately parametrized for atomic potentials in Ref. 30.

The importance of this scaling limit for DFT is not hard to discover: it is universal, applicable to any starting potential, and thus has universal consequences for DFT. Moreover, it rigorously probes perhaps the most important benchmark for DFT development, the periodic table.

#### 2. Application to neutral atoms

Lieb and Simon's  $\zeta$ -scaling takes on quantitative significance with the technique of asymptotic expansions of the energy of  $\zeta$ -scaled systems and in particular, of atoms versus  $Z^{-1}$  in the large- $Z$  limit.<sup>30–32,36–41</sup> Such expansions present the possibility of a direct systematic derivation of DFT approximations, as an expansion in a small parameter.<sup>32</sup> And, although proven rigorously for the difficult case of Coulomb-interacting systems, the results are straightforward to generalize to other, smoother potentials.<sup>49</sup>

Since all systems weakly tend to the TF energy and density in the Lieb-Simon ( $\zeta \rightarrow \infty$ ) limit, TF theory necessarily determines the leading order term in  $\zeta^{-1}$ , in the

asymptotic expansion for the energy. Corrections to the TF energy and density in the universal density functional must then appear in subsequent orders in the expansion. Fortunately, it is often the case that the higher the power of  $\zeta$  in the asymptotic series, the simpler the functional form that can contribute to it. This gives one a way to model corrections such as the gradient expansion (GE) in isolation, albeit with some complications for the Coulomb potential.<sup>51</sup> Ultimately, at  $\zeta = 1$ , the full complexity of DFT is revealed. Thus, we expect that contributions to each order in the expansion in  $\zeta$  can be captured by successively higher rungs in a mathematically derived Jacob's ladder of non-empirical approximations.

The power of this approach is revealed by its accuracy. Applied to neutral atoms, where  $\zeta$  is equal to the nuclear charge  $Z$ , and taking only the leading order Thomas-Fermi term in the asymptotic expansion of the total energy, one predicts the total energy of Rn within 3%, He to within 12%, and H to within 50% (and much better if spin-polarization is allowed for). The expansion behaves exactly as a perturbation expansion should – the leading order, though clearly not good enough for thermochemistry, gets the ballpark answer for *any*  $Z > 1$ , that is, the entire periodic table, and including even the next higher-order term makes the expansion much more accurate. Thus, the  $Z \rightarrow \infty$  limit provides the foundation of the description of matter for any  $Z$ .

Over the years,<sup>30–32,36–41,52,53</sup> the asymptotic expansion of the various contributions,  $T_s$ ,  $E_x$ ,  $E_c$  to the total energy in KS theory have been worked out for the case of atoms. In the limit  $Z \rightarrow \infty$  we have

$$\begin{aligned} T_s(Z) &= A_s Z^{7/3} - Z^2/2 + B_s Z + \dots, \\ E_x(Z) &= -A_x Z^{5/3} + B_x Z + \dots, \\ E_c(Z) &= -A_c Z \ln Z + B_c Z + \dots \end{aligned} \quad (5)$$

Here  $A_s \approx 0.768745$  as originally derived by Thomas and Fermi,<sup>52,53</sup>  $A_x \approx 0.220874$ ,<sup>30</sup> and  $A_c \approx 0.02073$ .<sup>32,41</sup> (We use atomic units (energies in hartrees) and give derivations for spin-unpolarized systems for simplicity.) As with the total energy, each leading order term is exactly given by the corresponding local density approximation in the high density limit, applied to the Thomas-Fermi density. For the kinetic energy, this is simply the Thomas-Fermi energy, constructed from an energy density that behaves as  $n^{5/3}(\mathbf{r})$ , for exchange, the LDA form  $\sim n^{4/3}(\mathbf{r})$  and for correlation, the high-density limit of LDA correlation.<sup>41</sup> Thus the LDA is the large- $Z$  limit for the single atomic potential and it is plausibly the universal large- $Z$  limit for electronic matter.

For correlation, the high density limit of LDA was derived by Gell-Mann and Brueckner<sup>54</sup> who applied the random phase approximation (RPA) to find:

$$\lim_{r_s \rightarrow 0} \epsilon_c^{\text{unif}} = \gamma \ln r_s + \eta, \quad (6)$$

where  $r_s = (3/(4\pi n))^{1/3}$  is the Wigner-Seitz radius of density  $n$ ,  $\gamma = 0.031091$ . Within the RPA,  $\eta = 0.07082$

and is 0.04664 in the exact high-density limit. (We use an accurate modern parametrization that contains these limits,<sup>55</sup> here and in construction of GGAs.) Then<sup>56</sup>

$$E_c^{\text{LDA}}[n] = \int d^3r n(\mathbf{r}) \epsilon_c^{\text{unif}}(n(\mathbf{r})), \quad (7)$$

which overestimates the magnitude of the correlation energy of atoms by a factor of two or more. Now apply Lieb-Simon scaling to this result, by inserting  $n_Z^{\text{TF}}(\mathbf{r})$  [Eq. (4)] and the high density limit for  $\epsilon_c^{\text{unif}}$  [Eq. (6)] into Eq. (7), to find:

$$E_c^{\text{LDA}} = -A_c Z \ln Z + B_c^{\text{LDA}} Z + \dots, \quad (8)$$

The leading term can thus be determined as  $A_c = 2\gamma/3 = 0.02073$ . The next term requires a numerical calculation over the TF unit density for atoms [Eq. (4)], yielding  $B_c^{\text{LDA}} = -0.00451$ .

Second-order terms require beyond-LDA density functional corrections whose strength depends on the properties of the potential being scaled.  $B_x$ <sup>31</sup> is entirely determined by the gradient expansion approximation (GEA) for slowly-varying densities, given by total energy:

$$E_x = E_x^{\text{LDA}} + \Delta E_x^{\text{GEA}}, \quad (9)$$

and energy per particle

$$\Delta \epsilon_x^{\text{GEA}} = \mu s^2 \epsilon_x^{\text{LDA}}, \quad (10)$$

with  $s = |\nabla n|/4k_F n$  a measure of inhomogeneity for exchange relative to the fermi wavevector  $k_F = (3\pi^2 n)^{1/3}$ . The validity of this form for atoms is justified by the fact that  $s^2$  scales as  $Z^{-2/3}$  under Lieb-Simon scaling so that higher-order gradient corrections such as  $s^4$  vanish relative to it. However, the value for  $\mu$  is different for potentials with and without a Coulomb singularity – that<sup>57</sup> of a sinusoidal potential (10/81) is roughly half that which is obtained by extrapolating the exchange energy of atoms to the large  $Z$  limit.<sup>26,31</sup> This discrepancy explains the frequent rejection in modern GGAs (both empirical and non-empirical) of the formally derived parameter of 10/81 for values that approach that of the large- $Z$  limit.<sup>31</sup>

### 3. Correlation: Determining $B_c$

The second-order term for correlation,  $B_c$  is much harder to determine than  $B_x$  because it is nearly the same order of magnitude as the leading correlation term and thus hard to extract from atomic data. Moreover, as discussed in the next section where we delineate the careful construction of a high-density GGA, the gradient expansion (GE) alone does not suffice to describe this coefficient. At a minimum a GGA is required. Nevertheless recent work has determined an accurate estimate of  $B_c$ ,<sup>32</sup> based on coupled-cluster calculations for closed-shell atoms up through  $Z = 86$ ,<sup>44</sup> and all atoms up

through  $Z = 54$ .<sup>45</sup> These, along with the earlier benchmark set<sup>58</sup> have made possible a reasonably accurate extrapolation of  $B_C$ .

It will be important to describe the extrapolation method in detail as it generates a benchmark that we use to produce an asymptotically correct GGA. As  $A_C$  is exact for atoms,<sup>41</sup> we reformulate the asymptotic expansion to define the target for any beyond-LDA DFT:

$$B_C = \lim_{Z \rightarrow \infty} e_{AC}(Z), \quad e_{AC}(Z) = \frac{E_C(Z)}{Z} + A \ln Z, \quad (11)$$

or alternatively as

$$\Delta B_C = B_C - B_C^{\text{LDA}} = \lim_{Z \rightarrow \infty} \frac{[E_C(Z) - E_C^{\text{LDA}}(Z)]}{Z}. \quad (12)$$

A natural procedure to eliminate the effects of shell structure is to consider the trend down a specific column of closed shell atoms like the noble gases. One may find an even smoother trend by averaging over closed shells across a single row, as described in Ref 32. The results are conveniently parametrized versus the inverse of the row number (which we take to be the principle quantum number of the highest occupied energy shell,  $n_{\text{HOMO}}$ .)

The result of this procedure is shown in Fig. 1, and is compared to the predictions of several GGA functionals. The GGA functionals are calculated out to  $n_{\text{HOMO}} = 11$ , ignoring issues of nuclear stability, in order to verify their convergence properties in the Lieb-Simon limit. We see that PBE trends quickly to a  $Z \rightarrow \infty$  value of  $\Delta B_C = 43.87$  mHa determined by applying the TF density to the beyond-LDA component of PBE. In comparison,  $B_C$  for the LYP<sup>59</sup> clearly diverges, and that of P86,<sup>47</sup> while finite, falls off from the QC trend. PBE closely parallels the QC data, and assuming that electronic structure effects grow smaller for larger  $Z$ , this parallel is hypothesized to continue on to the  $Z \rightarrow \infty$ ,  $1/n_{\text{HOMO}} \rightarrow 0$  limit. The difference may be fit to a straight line trend,

$$\frac{(E_C - E_C^{\text{PBE}})}{Z} = -0.00220(38) + \frac{0.0002(13)}{n_{\text{HOMO}}}. \quad (13)$$

Thus  $\Delta B_C^{\text{QC}} = 41.7$  mHa, shown as the second horizontal line in Fig. 1.<sup>60</sup> This formula becomes a smooth function of  $Z^{1/3}$  as  $Z \rightarrow \infty$  (the difference in  $Z$  between an alkali earth or noble of the same row disappears relative to  $Z$  in this limit) and being a constant, should be largely independent of specifics of the parametrization method. It clearly reproduces trends in the QC data beyond our initial target,  $B_C$ . In fact, we make a reasonable guess at the smooth contribution of all the higher-order terms in the asymptotic series.

The goal of the current paper is the natural followup of this result – to understand why PBE correlation works as well as it does, and then make it asymptotically correct. It allows us to make a precise (though not exact) definition of asymptotically correct at the level of a GGA. The asymptotically corrected functional should recover

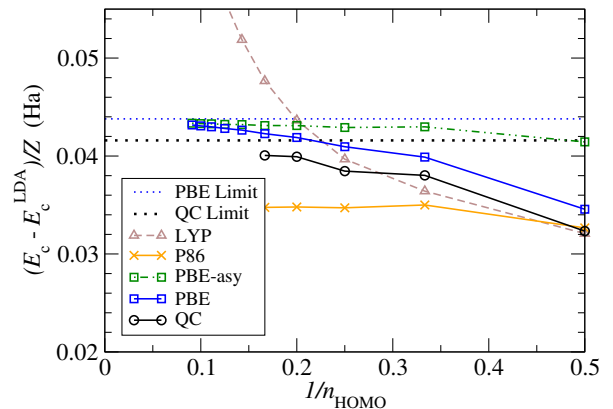


FIG. 1. Beyond LDA contribution to the correlation energy per electron for several GGA approximations compared to accurate quantum chemistry calculations (QC), averaged over the alkali earth and noble gas atoms of each row of the periodic table and plotted versus inverse row number TF shows the asymptotic limit of PBE,  $B_C^{\text{PBE}}$ , and PBE-asy is the  $r_s = 0$  limit of PBE evaluated with a self-consistent Kohn-Sham density.

the correct value of  $B_C$ , and as far as possible, do so by repeating the smooth asymptotic trend to low  $Z$  extracted from QC data. Thus we have a benchmark that a GGA can be expected to match – the smooth asymptotic trend with  $Z$  of the periodic table, eschewing the full details of atomic electronic structure, or the complexities of covalent bonding of molecules.

## B. How (and why) PBE correlation works

In order to understand why PBE should be accurate in the Lieb-Simon limit, we review the history of non-empirical GGAs. A major role is played by the real-space cutoff (RSC) model of the exchange-correlation hole which functions as the equivalent of a norm used to generate the PBE and impose the constraints which it satisfies. We also note ambiguities in the high-density limit of RSC that will guide our correction to the PBE.

### 1. The gradient expansion for correlation

A first step in developing a nonempirical GGA for correlation is the derivation within the RPA by Ma and Brueckner (MB) of the leading gradient correction for the correlation energy of a slowly-varying electron gas.<sup>61</sup> Define

$$\Delta E_C = E_C - E_C^{\text{LDA}} = \int d^3r n(\mathbf{r}) H_C [r_s(\mathbf{r}), t(\mathbf{r})], \quad (14)$$

where  $t = |\nabla n|/(2k_s n)$  is a dimensionless measure of inhomogeneity appropriate for correlation, and  $k_s = 2(3n/\pi)^{1/6}$  is the TF screening wavenumber.<sup>3</sup> The MB

gradient expansion approximation yields

$$H_C^{\text{GEA}}(t) = \beta t^2, \quad (r_s \rightarrow 0) \quad (15)$$

with  $\beta = 0.066725$ . This so strongly overcorrects  $E_C^{\text{LDA}}$  for atoms<sup>61</sup> that we find that  $E_C$  becomes positive for all atoms. MB showed that a simple Padé approximant works much better, creating the first correlation GGA, and inspiring the work of Langreth and Perdew,<sup>62</sup> among others.

We can apply Lieb-Simon scaling to the gradient expansion to show *a priori* the unsuitability of the GE for the density functional description of correlation, and thus the need for a GGA. As  $Z \rightarrow \infty$ , the GE applied to the TF density scales as  $Z \ln Z$ , not  $Z$ , giving a spurious gradient correction to  $A_C$  in the asymptotic expansion, as shown in Appendix A. Only a GGA gives a gradient correction that scales correctly. The divergent behavior in the LYP estimate of  $B_C$  seen in Fig. 1 is in part caused by the use of the simple gradient expansion form. At small  $Z$ , the GE corrections are tempered by deviations from the homogeneous electron gas form of the LDA to produce an excellent description of correlation, but the cost is a necessary failure at large  $Z$ .

## 2. Real-space hole construction of the GGA

Underlying the PBE and related GGAs is the non-empirical real-space cutoff (RSC) model for the XC hole<sup>5,63,64</sup>, so we review it in detail. It will serve as the foundation for asymptotically correcting PBE.

The XC hole is defined as

$$n_{\text{XC}}(\mathbf{r}, \mathbf{r}') = \int_0^1 d\lambda (P_\lambda(\mathbf{r}, \mathbf{r}')/n(\mathbf{r}) - n(\mathbf{r}')) \quad (16)$$

where  $P_\lambda(\mathbf{r}, \mathbf{r}')$  is the pair probability density at coupling constant  $\lambda$  along the adiabatic connection curve. Then

$$E_{\text{XC}} = \frac{1}{2} \int d^3r \int d^3r' \frac{n(\mathbf{r}) n_{\text{XC}}(\mathbf{r}, \mathbf{r}')}{|\mathbf{r} - \mathbf{r}'|}. \quad (17)$$

It is interpreted as a change in density at  $\mathbf{r}'$  given an electron observed at  $\mathbf{r}$ , and may be constructed by taking the adiabatic integral over coupling constant for this quantity.<sup>65–67</sup>  $E_{\text{XC}}$  does not depend sensitively on the details of the XC hole, but rather on its system and angle average:

$$E_{\text{XC}} = \frac{1}{2} \int 4\pi u^2 du \frac{1}{u} \langle n_{\text{XC}}(u) \rangle \quad (18)$$

with  $u = |\mathbf{r} - \mathbf{r}'|$ , and the average is over the other coordinates in Eq. 17. The XC hole obeys important normalization sum rule that  $\int d^3r' n_{\text{XC}}(\mathbf{r}, \mathbf{r}') = -1$  while the correlation hole alone obeys  $\int d^3r' n_c(\mathbf{r}, \mathbf{r}') = 0$ .

The LDA can be considered as approximating the true XC hole by that of a uniform gas:

$$n_{\text{XC}}^{\text{LDA}}(\mathbf{r}, \mathbf{r}') = n(\mathbf{r}) [\bar{g}^{\text{unif}}(r_s(\mathbf{r}), |\mathbf{r} - \mathbf{r}'|) - 1] \quad (19)$$

where  $\bar{g}^{\text{unif}}$  is the pair-correlation function of the uniform gas.<sup>68</sup> Insertion of this approximate hole into Eq. (17) yields  $E_{\text{XC}}^{\text{LDA}}[n]$ . While  $\epsilon_{\text{XC}}^{\text{unif}}(n(\mathbf{r}))$  is not accurate point-wise,<sup>69</sup> (that is, it is not comparable to the integral over  $r'$  in Eq. 17) the system and angle average of the LDA hole is. This is because the LDA hole satisfies basic conditions – it obeys the particle sum-rules for both exchange and correlation and satisfies the negativity condition for exchange,  $n_x(\mathbf{r}, \mathbf{r}') \leq 0$ . So it mimics the exact hole. Conversely, the exact  $E_{\text{XC}}$  depends only upon the system average of the exact hole, and this is insensitive to details of electronic structure of an inhomogeneous system, so capturing these major features suffices. Hence the reliability and systematic errors of LDA.<sup>69</sup>

XC hole analysis also shows why the gradient expansion fails:  $n_{\text{XC}}^{\text{GEA}}$  for a sufficiently rapidly varying system has large unphysical corrections to  $n_{\text{XC}}^{\text{LDA}}$ , violating the exact conditions that the LDA obeys.<sup>70</sup> For correlation, the correction to the LDA hole<sup>63</sup> is proportional to  $t^2$  and positive definite, a response to the averaged exchange hole, which becomes deeper and more localized, and therefore more efficient at screening. The GEA hole thus must break the normalization sum rule for correlation for any non-zero  $t$ , and do so drastically for situations in which  $t^2$  diverges.

By restoring these exact conditions, the RSC construction determines the very difficult and essentially nonlocal piece of information needed to reproduce the hole of an atom or molecule – its finite range. For correlation, the GEA hole is made to satisfy the zero sum-rule by cutting it off outside a finite radius  $v_c$ . This crude procedure is surprisingly effective at predicting the finite range of real holes, while the GEA hole is typically very good at small interparticle distances, dramatically improving upon the LDA hole in this limit.<sup>71</sup>

## 3. Constraints derived from the real-space cutoff

The RSC model, through Eq. 17, defines a numerical GGA that naturally generates the properties and constraints that PBE and related functionals attempt to meet, and suggests a robust functional form. In this sense, it can be considered the generator of PBE and motivates our using it to generate its correction. The constraints can be separated into the high density limit  $r_s = 0$ , of immediate interest to us, and those that impose corrections for finite  $r_s$ .

In the  $r_s = 0$  limit, and at low  $t$ , the RSC by construction reduces to the Ma-Brueckner GE form, Eq. (15). At high  $t$ , typical of a finite system, the RSC cut-off procedure removes the logarithmically divergent LDA energy term in Eq. (6),  $\gamma \ln r_s$ , yielding a finite  $E_C$ . This is the limit reached by the uniform scaling of the density of any finite system to high density, here the correlation energy is constrained to be bounded from below.<sup>72,73</sup> RSC also gives a physically reasonable interpolation between the two for finite  $t$ .

At finite density, the low- $t$  limit also reduces to the Ma-Brueckner gradient expansion, ignoring the weak dependence of the coefficient  $\beta$  on  $r_s$  calculated by Langreth and coworkers<sup>62,74</sup> and Rasolt and Geldart.<sup>75,76</sup> The high- $t$  limit yields a diverging GEA correlation hole with a sum rule so unphysically positive that the RSC procedure cuts it off almost entirely. This yields an  $E_C$  that vanishes as  $1/t^2$ ,<sup>64</sup> satisfied by requiring  $H_C(r_s, t \rightarrow \infty) \rightarrow -\epsilon_C^{\text{LDA}}$ . At very low density, such as the asymptotic tail of a finite system, this limit is reached for almost any value of  $t$ . For atoms, it may be helpful to think of this as the finite- $t$ , low density ( $r_s \rightarrow \infty$ ) limiting case, complementary to the  $r_s = 0$  limit discussed above. The PBE correlation functional, like its predecessor PW91,<sup>19,64</sup> is based on a simple analytic parametrization of this numerical GGA, and attempts to capture not only its limit cases but the entire range of dependence on  $r_s$  and  $\zeta$ .

In the high density limit, the correction to the LDA reduces to a function of the single variable  $t$ , and both PBE and PW91 use the simplest possible form that can satisfy both high- and low- $t$  limits:

$$H_C(0, t) = \gamma \ln(1 + T^2), \quad (20)$$

defined in terms of a rescaled inhomogeneity parameter:

$$T = \sqrt{\frac{\beta}{\gamma}} t. \quad (21)$$

PW91 adds a second piece to the RSC correlation, in order to ensure a zero exchange-correlation correction in the linear response limit. Unfortunately, this term reduces to the gradient expansion in the  $r_s \rightarrow 0$  limit, and like the gradient expansion diverges unphysically. We drop this second piece in our discussion.

Fig. 2 shows  $H_C$  as a function of  $t$  for PBE and the RSC contribution to PW91, in comparison to the numerical RSC. The PW91 adjusts  $\gamma$  from the RPA value by a modest amount so as to give a close match to the numerical RSC at finite  $t$ . In doing so it sacrifices the constraint of a finite correlation energy at high  $t$ . In contrast, PBE preserves Ma-Brueckner low- $t$  correlation and the RPA value for  $\gamma$ . But greater attention to the limiting values of  $t$  within this restricted form creates a modest mismatch with the RSC at finite  $t$ . The PBE is thereby justifiable purely on constraints in *limiting* cases, obviating ultimately the need for reference to the XC hole.

At finite  $r_s$ , the analytic parametrization of the RSC generalizes to

$$H_C^{\text{PBE}}(r_s, t) = \gamma \ln(1 + T^2 f_C(y)). \quad (22)$$

This defines a cutoff function  $f_C(y)$  with a form

$$f_C(y) = (1 + y)/(1 + y + y^2), \quad (23)$$

where

$$y = a(r_s)T^2 \quad (24)$$

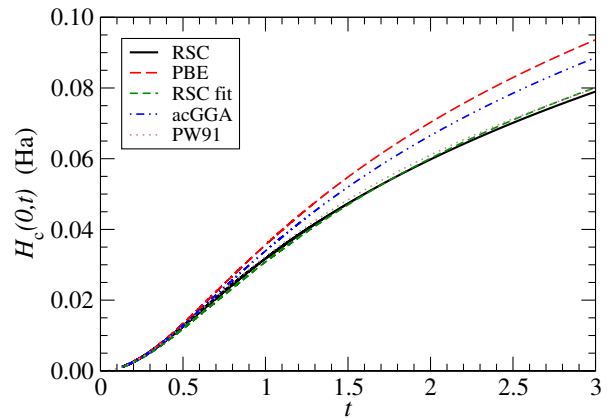


FIG. 2. The asymptotic ( $r_s = 0$ ) of the beyond LDA component  $H_C(0, t)$  for generalized gradient approximations, including the the real-space cutoff (RSC), the RSC contribution to PW91, PBE, our fit to the RSC using Eq. (30), and the asymptotically corrected GGA (acGGA).

identifies the transition between high and low density behaviors, and the form of  $f(y)$  approximates the behavior of the numerical RSC. It determines  $a(r_s)$  implicitly by enforcing zero net correlation energy in the large  $y$  limit:

$$H_C(r_s \rightarrow \infty, t) = \gamma \ln(1 + T^2/y) = -\epsilon_C^{\text{LDA}}(r_s) \quad (25)$$

which is satisfied by

$$a(r_s) = \{\exp[-\epsilon_C^{\text{LDA}}(r_s)/\gamma] - 1\}^{-1} \quad (26)$$

The function  $a(r_s)$  is roughly linear in  $r_s$ , so that  $y \sim s^2$ , the scale invariant exchange inhomogeneity parameter.

Before moving on, we consider the message of the RSC asymptotic form Eq. (20). Early correlation functionals, such as LYP but also Perdew 86<sup>47</sup> and Langreth-Mehl<sup>46</sup>, experimented with a wide variety of forms in this limit, but lacked knowledge of the proper limit of correlation in the limit of uniform scaling to high density, with  $r_s \rightarrow 0$  and  $t \rightarrow \infty$  simultaneously. The result was either a divergence in this limit for LYP, or a rather poor estimate for  $B_C$ , 31.0 mHa for Perdew 86. The part of PW91 that is based on the RSC improves upon the LDA in this limit, improving  $B_C$  to 34.6. PBE drops the divergent part of PW91 and fully implemented the uniform limit, yielding a nearly correct  $B_C$  of 39.38. What we need ( $\sim 37.2$ ) is a modest improvement upon what is already provided in Eq. (20) by enforcing the correct constraint under uniform scaling.

### III. CONSTRUCTING A NEW HIGH DENSITY GGA

In this section we show how the PBE construction fails to fully determine the leading correction to LDA in the Lieb-Simon limit for correlation. This correction can be folded in to PBE correlation, while still respecting all conditions PBE correlation was designed to satisfy. We also show how including density-dependence in this limit

is largely irrelevant, so we do not do so in our acGGA. Finally, we discuss which exchange GGA should be coupled with acGGA.

### A. The high- $Z$ limit of the GGA

We begin by exploring the implication of taking the combination of the high-density limit of the RSC model *and* high- $Z$  together. To do so, we define an asymptotic PBE by taking the high density limit of PBE for all densities,

$$\epsilon_c^{aPBE}(r_s, t) = -\gamma \ln r_s + \eta + H_c^{aPBE}(r_s, t) \quad (27)$$

where the first two terms are the high density limit of the LDA [Eq. 6], and the GGA correction is

$$H_c^{aPBE}(r_s, t) = \gamma \ln(1 + T^2), \quad (28)$$

applied for all  $r_s$ . We include calculations using this form in Fig. 1.

The coefficient  $B_c^{PBE} = 39.36$  mHa for PBE is simply the expectation of this high-density form of PBE using the TF density, and is shown as a dotted line. This term *alone* predicts the full self-consistent PBE model within 80% down to  $Z = 4$  ( $n_{\text{HOMO}} = 2$ ), showing the power of asymptotic analysis. Evaluated with self-consistent densities, aPBE (green squares) gives the correction to  $B_c$  due to the change in density from TF case. This is seen to be a small effect for all  $n_{\text{HOMO}}$ . The difference of aPBE and PBE shows the effect of the finite-density correction to  $H_c$ , and naturally turns on mostly for the first two values of  $n^{\text{HOMO}}$ . But crucially, it is almost perfectly zero for larger  $Z$ , where the small change due to the change in density is dominant. The low-density correction of PBE is only relevant for the lowest rows of the periodic table and QC data mimics this behavior closely. Changing  $B_c$  alone, i.e., modifying aPBE to retrieve the QC value of  $B_c$  (black dotted line) promises therefore to reproduce the QC values for most of the periodic table.

Secondly, we illuminate the nature of the asymptotic constraint we wish to use and how it affects the form of the GGA. Take the asymptotic expansion coefficient  $\Delta B_c$  as expressed by Eq. (12), and the value for it, 0.0417 Ha, extrapolated from QC data. Insisting that this condition be met by a GGA with gradient correction given by the general form of Eq. (14) leads to the following constraint

$$\frac{1}{Z} \int d^3r n_Z^{\text{TF}}(\mathbf{r}) H_c(0, t[n_Z^{\text{TF}}(\mathbf{r})]) = B_c - B_c^{\text{LDA}} \sim 0.0417 \quad (29)$$

where  $B_c^{\text{LDA}} = -0.00451$  and  $n_Z^{\text{TF}}$  is given by Eq. (4). We examine the values of  $t$  that contribute to this integral, by changing the integration variable in Eq. (29) to  $t$  to obtain the function  $dB_c/dt$ , shown in Fig. 3. The curve as shown thus integrates to  $B_c$ . The GEA is clearly too large in magnitude and has a slowly decaying  $1/t$  tail that

leads to a logarithmic divergence. The RSC asymptotic form implemented in PBE removes most of the correction of the GEA and particularly the high- $t$  tail. It thus obtains a distribution strongly peaked around  $t \sim 0.9$ , no values of  $t$  smaller than 0.72, and a rapidly decreasing tail for  $t > 1$ , with a greater than 95% contribution to  $B_c$  for  $t < 5$ . Thus  $B_c$  basically pins down the value of  $H_c(0, t)$  for the characteristic Thomas-Fermi value of  $t \sim 1$ . The needed asymptotic correction is a small ( $\sim 5\%$ ) reduction of this curve in order to reduce  $B_c$ ; and the solution we describe below, the acGGA, is shown here as well.

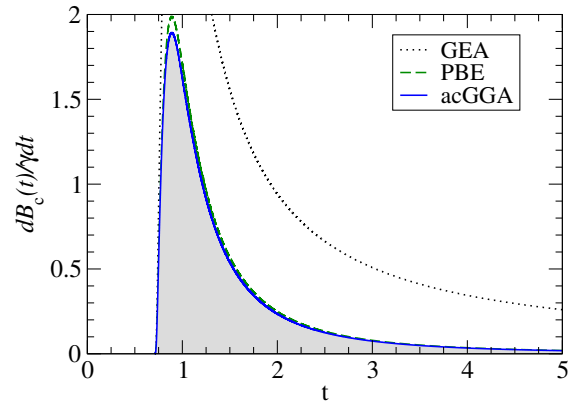


FIG. 3. Plot of  $B_c$  represented as an integral over the inhomogeneity parameter  $t$ . Obtained parametrically by plotting  $4\pi r^2 n(r) H_c(0, t(r)) / (\gamma dt/dr)$  versus  $t(r)$  evaluated for the TF density. Green dashed line represents the asymptotic limit of PBE; black dotted, the GEA; blue, the acGGA. Shaded area is the integral  $B_c^{\text{acGGA}} - B_c^{\text{LDA}}$ .

In contrast, asymptotic scaling for exchange tells us about  $s \rightarrow 0$ :  $s \sim \sqrt{r_s} t$  and goes to zero for finite  $t$  as  $r_s \rightarrow 0$ . Asymptotic analysis of this limit conflicts with the conventional small- $s$  expansion about the uniform gas,<sup>57</sup> indicating why disagreement with *a priori* calculations proved desirable for density functional description of real systems.<sup>28,31</sup> Asymptotic scaling for correlation tells us about  $t \sim O(1)$ , a genuinely new piece of information in addition that of the limit of uniform scaling to high density, and the gradient expansion. Thus it does not necessarily conflict with prior results, indicating why keeping the Ma-Brueckner gradient expansion for correlation was not a problem for the development of realistic density functionals.

### B. Correcting the high- $Z$ limit of PBE

As discussed above, we expect that correcting the leading order term  $B_c$  in the asymptotic expansion for correlation will play a dominant role in reducing the PBE correlation error for all  $Z$ . On the other hand, the accuracy of  $B_c^{PBE}$  suggests the real-space cut-off procedure from which it derives is highly accurate at high density. We thus construct an asymptotically correct GGA by extending the analytic RSC form to give flexibility to match



low- $t$ , high- $t$  and  $t = 1$  behaviors independently. We do this by modifying Eq. (20) to

$$H_C^{\text{acGGA}}(0, t) = \gamma \ln(1 + P(t)T^2), \quad (30)$$

where

$$P(t) = (1 + t/\tau)/(1 + \tilde{c}t/\tau). \quad (31)$$

To determine a suitable choice of parameters for  $P$  we first fix both  $\tau$  and  $\tilde{c}$  to match the numerical RSC without the limitations of Eq. (20). Keeping both the large- $t$  coefficient  $\gamma$  and small- $t$  coefficient  $\beta$  at the RSC values, we match the second order term in the RSC large- $t$  limit – the finite constant that is left after cancelling the spurious  $\ln r_s$  divergence in the LDA correlation. As derived in Appendix B, this condition is satisfied by  $\tilde{c} = 2.4683$ . We then set  $\tau = 4.5$  to match the RSC curve at finite  $t$ , and show the result, labeled “RSC fit” in Fig. 2. This model yields a value of  $B_C^{\text{RSC}}$  of 0.0327, somewhat off from our extrapolated value, and reflects the uncertainty in RSC in this limit.

To construct an approximation without this uncertainty, we keep  $\tau$  the same, but choose  $\tilde{c}_{\text{AC}} = 1.467$ , which reproduces our best estimate of  $B_C = 0.0372$ .<sup>77</sup> This result, an asymptotically correct GGA, lies between the RSC and PBE GGAs, as shown in Fig. 2. This indicates the good quality of the original RSC for finite  $t$ , but also indicates that the PBE was a step in the right direction.

We make  $P(t)$  a function of  $t$  not  $t^2$  in order to match the high- $t$  limit. This alters the low- $t$  gradient expansion, producing a new term proportional to  $t^3$ . The practical effect of this is very small for the asymptotically correct model for  $P(t)$  ( $\tilde{c}_{\text{AC}}$ ) as the third-order coefficient is nearly zero.

### C. Extension to finite density

To construct an acGGA good for finite  $r_s$  we define

$$\epsilon_C^{\text{acGGA}}(r_s, t) = \epsilon_C^{\text{LDA}}(r_s) + H_C^{\text{acGGA}}(r_s, t), \quad (32)$$

where

$$H_C^{\text{acGGA}}(r_s, t) = \gamma \ln\left(1 + \tilde{T}(t)^2 f_C(\tilde{y})\right), \quad (33)$$

$$\tilde{T} = \sqrt{P(t)}T. \quad (34)$$

Enforcing the low density finite- $t$  limit [26] now requires

$$\tilde{y} = a(r_s)\tilde{T}(t)^2. \quad (35)$$

That is, we have simply replaced  $T$  by  $\tilde{T}(t)$  everywhere in the PBE. We now have an acGGA that meets all the constraints previously met by PBE as well as the new condition of asymptotic correctness under Lieb-Simon scaling to  $Z \rightarrow \infty$ .

To see how well the acGGA reproduces the smooth asymptotic trend defined by Eq. (13), we first plot this trend versus  $1/n_{\text{HOMO}}$  in Fig. 4. The difference between QC and PBE correlation energies per electron averaged over closed shells in each row – the data to which this trend is fit – is also shown to give a sense of the error of the fit. We compare these to the difference between acGGA and PBE correlation energies per electron averaged over closed shells in the same way as the QC data. These are computed self-consistently up to  $n_{\text{HOMO}} = 11$ , and an extrapolation to  $n_{\text{HOMO}} \rightarrow \infty$  is done by calculating this averaged energy difference using the Thomas-Fermi density. These are shown in Fig. 4 as blue circles and blue dashed line, respectively. Energies determined using the Thomas-Fermi density clearly converge to the extrapolated  $B_C$  value in the  $n_{\text{HOMO}} \rightarrow \infty$  limit, and are very close to the self-consistent ones for large  $n_{\text{HOMO}}$ . This provides confirmation that the self-consistent acGGA is in fact trending to  $B_C \sim 37.1$  mHa as designed.

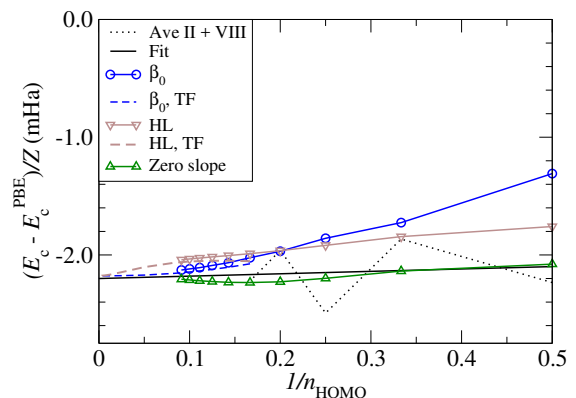


FIG. 4. Difference between the correlation energy-per-electron of the acGGA and PBE averaged over noble gas and alkali earth atoms, plotted versus  $1/n_{\text{HOMO}}$ , compared to asymptotic extrapolation from QC data. Dotted black line shows QC average for  $n_{\text{HOMO}} = 2$  through  $n_{\text{HOMO}} = 6$ , excepting Ne. Solid black is the smooth asymptotic curve Eq. (13). Blue circles are acGGA, using the  $r_s = 0$  value of  $\beta$ , evaluated self-consistently through  $n_{\text{HOMO}} = 11$ ; blue dashed line, their extension to  $n_{\text{HOMO}} \rightarrow \infty$  on the TF density. Brown triangles and long-dashed line, acGGA-HL, using the Hu-Langreth  $\beta(r_s)$ ; green triangles, acGGA+, a modification of HL with  $d\beta/dr_s = 0$  at  $r_s = 0$ .

We also note how close the acGGA data is to a smooth curve after performing our averaging process – the effects of shell structure are more than an order of magnitude smaller than that of the averaged QC data. This validates our intuition that the appropriate norm to match a GGA against is not the atomic data itself, even when restricted to a single column of the periodic table, but the smooth asymptotic trend derived from that data.

However, while the acGGA correction faithfully follows the asymptotic trendline at the highest densities, at finite densities it gradually lifts off the trendline deviating especially in the “last” three rows of the “inverse” periodic

table where it is off by a fraction of a mHa per electron. Simply fixing  $B_C$  removes 90% of the difference between PBE and our smooth asymptotic trend for  $n_{\text{HOMO}} = 6$ , but only 60% for  $n_{\text{HOMO}} = 2$ .

The modest failure of our first try at an acGGA has a relatively easy explanation and fix. It is the necessary connection between the modified variable  $\tilde{T}$  used to generate the high density limit of  $H_C^{\text{acGGA}}$  and the modified variable  $\tilde{y}$  used in the cutoff function  $f_C(\tilde{y})$  that determines when PBE crosses over to its low density, finite- $t$  limit. At highest  $Z$ , when  $r_s$  is nearly but not exactly zero, the cutoff function  $f_C$  makes very nearly no change to the correlation energy. This leads to the flat plateau seen in Fig. 4 for  $E_C^{\text{acGGA}} - E_C^{\text{PBE}}$  as  $1/n_{\text{HOMO}} \rightarrow 0$ . When  $r_s$  gets sufficiently small, the replacement of  $y$  in PBE by  $\tilde{y}$  in the acGGA results in a weaker cutoff because  $\tilde{T}$  has been made smaller than  $T$  in order to reduce  $B_C$  from the PBE value. And thus, on average, PBE correlation will shut off faster than the acGGA, leading to the rise of the latter relative to the former.

To improve the behavior of the acGGA at finite  $r_s$ , a sufficient step is to impose more carefully the  $r_s$  dependence of the GE for correlation, left unimplemented in PBE. This correction yields an  $r_s$ -dependent  $\beta$  coefficient to the gradient expansion [Eq. (15)], with  $\beta(0)$  equal to the Ma-Brueckner value. It has been calculated by two groups,<sup>74,75</sup> yielding similar results. This  $r_s$  dependence is rather modest (as shown below) but recent meta-GGAs<sup>2,15</sup> have found it useful for fine-tuning correlation. At the level of fine-tuning remaining to adjust the acGGA, it proves to be a significant effect.

The original Hu-Langreth (HL) form is numerical but we parametrize it roughly along the lines used in revTPSS<sup>15</sup> to obtain

$$\beta(r_s) = \beta(0) \frac{1 + ar_s(b + cr_s)}{1 + ar_s(1 + dr_s)}. \quad (36)$$

The coefficients  $a = 3.0$ ,  $b = 1.046$  and  $c = 0.100$  approximately match the HL form for  $r_s < 1$ . The high- $r_s$  limit for  $\beta$ , however, is unlikely to be that given by the HL calculation, and instead we use the limiting condition defined by revTPSS, setting the ratio  $c/d = 1/1.778$ . We also consider a model with zero slope in  $\beta(r_s)$  as  $r_s \rightarrow 0$ , closer in form to that of Ref. 75, with coefficients  $a = 0.5$ ,  $b = 1$ ,  $c = 0.16667$ ,  $d = 0.29633$ . These models for  $\beta(r_s)$  are shown in Fig. 5, compared to the one used in revTPSS. They roughly compare in slope but differ somewhat in magnitude because of the differing behavior near  $r_s = 0$ .

The effect of  $r_s$  dependence in the GE is to alter the high-density limit of the acGGA to the form  $H_C^{\text{asy}}(r_s \rightarrow 0, t) = \gamma \ln(1 + \tilde{T}(r_s, t)^2)$ , where

$$\tilde{T}(r_s, t) = \sqrt{P(t)} \sqrt{\beta(r_s)/\gamma} t \quad (37)$$

is the same as  $\tilde{T}(t)$  [Eqs. (34) and (21)] but now using an  $r_s$ -dependent expression for  $\beta$ . A similar change to  $\tilde{y}$  adjusts the transition to the low density form. The key

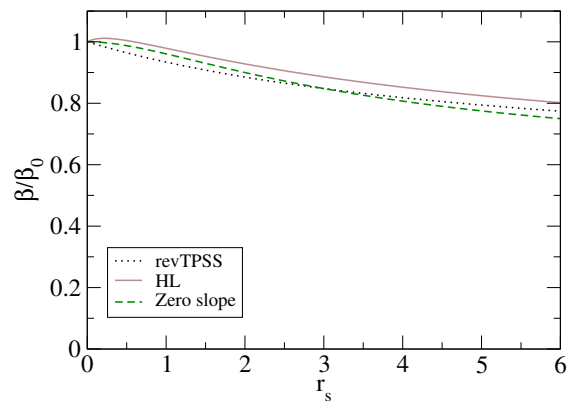


FIG. 5. Relative variation in the gradient expansion coefficient  $\beta$  as a function of  $r_s$ . revTPSS is the model introduced in Ref. 15. The other two are implementations of Eq. 36 discussed in the text: HL reproduces the model of Ref. 74 and “Zero-slope” is designed for close reproduction of Eq. 13.

here is that this generalizes  $B_C$  into a weak function of  $r_s$ . For high  $Z$ , the slope of  $B_C(r_s)$  is linearly proportional to that of  $\beta(r_s)$  and this offers a way to tailor the acGGA’s functional dependence on  $r_s$ .

As  $\beta(r_s)$  generally tends to decrease, the outcome for either the HL or zero-slope model is to lower the effective  $B_C(r_s)$  of the acGGA relative to PBE. This pleasingly cancels the trend away from our target asymptotic line, so we end up more closely matching QC correlation energies in the first few rows of the periodic table, as shown in Fig. 4. However, in the HL gradient expansion, the slope in  $\beta(r_s)$  at  $r_s = 0$  is *positive*, increasing  $\beta(r_s)$  at high density and lifting the modified acGGA off the asymptotic line used to measure  $B_C$ . This lift makes it impossible to match the asymptotic line without readjusting  $B_C$  by at least a few tenths of a mHa. In contrast, the model with zero slope at  $r_s = 0$  almost perfectly matches the asymptotic line. We thus take the zero-slope model for  $\beta(r_s)$  applied in Eqs. (37) and (33) as a modified acGGA, denoted acGGA+.

#### D. Asymptotically correct exchange

In order to minimize the overall error in XC, we apply asymptotic methodology to exchange as well. There is a fundamental difference between  $\zeta$ -scaling of exchange and correlation. The parameter  $s^2$  that determines the gradient correction for exchange scales to zero as  $\zeta \rightarrow \infty$ , while  $t^2$  is invariant under  $\zeta$ -scaling and even at  $\zeta \rightarrow \infty$  spans a wide range of values seen in Fig. 3. Thus the asymptotic limit of exchange may be used to generate appropriate coefficients for a gradient expansion, but does not inform the entire character of a GGA as we have been able to do for correlation. Thus one finds the lowest order coefficient for exchange to be  $\mu = 0.2603$ , in contrast to the formal gradient expansion result of  $10/81$ . and recent asymptotic analysis suggests a fourth order cor-

rection of  $-0.125s^4$ .<sup>26</sup> Notably, any exchange functional that predicts accurate energies for atoms uses a value of  $\mu$  close to that predicted by asymptotic analysis, with small variations to capture higher order expansion terms for finite- $Z$  atoms. Conversely, asymptotic analysis is irrelevant to the large  $s$  limit of exchange GGAs, and exchange functionals with very different behavior in this limit can have desirable thermochemical properties.<sup>26,27</sup>

Most exchange functionals, including the commonly used B88<sup>78</sup> and PBE, are already reasonably asymptotically accurate for exchange.<sup>31</sup> For simplicity, we limit our study to these two forms. Table 1 of Ref. 31 shows a small underestimate in the coefficient from PBE, but we can correct for this by increasing  $\mu$  in the formula for  $E_x^{\text{PBE}}$  by 13%, to 0.249. We label this acPBEx, denoting modified PBE exchange. Either acPBEx or B88 make an attractive candidate to pair with acGGA correlation, so we test both forms below. We will take B88 exchange plus acPBE correlation to be the normative acGGA, B88 with acGGA+ correlation as acGGA+, and label acPBEx combined with acGGA as P-acGGA.

#### IV. MEASUREMENTS AND TESTS

In this section, we take the final acGGA formulas and show their errors on the neutral atoms (for which they've been designed to be increasingly accurate with increasing atomic number). But we also test acGGA on atomization energies, including attempts to construct hybrids from acGGA.

##### A. Atoms

We first explore the behavior of the acGGA and acGGA+ across the entire periodic table. Complete quantum chemistry data is available for the first four rows  $p = 1$  to 4 of the periodic table but only for closed shells for  $Z > 54$ . To augment the available test set for  $p = 5$  and 6, we replace the QC data for closed shell atoms with asymptotically corrected RPA (acRPA) data<sup>32</sup> that very nearly duplicates it, and fill in acRPA data for the open-shell atoms in these rows. The errors in acRPA data are shown in Table I, and are much smaller than the difference between acRPA and any functional tested. For reference exchange energies, we take EXX calculations using the OPMKS code.<sup>79</sup>

The left side of Table I lists errors averaged over row of the periodic table for atomic correlation energies with respect to this reference set. LDA overestimates by about 1 eV per electron, consistent with its error for  $B_C$ . PBE reduces this error by about a factor of 10, consistent with its almost exact value for  $B_C$ . But, by being exact for  $B_C$ , acGGA reduces this error by a further factor of 2. The empirical LYP does best for  $Z < 10$ , vital to organic chemistry, but is substantially worse past period 3. We see the density dependence in acGGA+ yields no overall

improvement relative to acGGA, but does do better for the second row.

For XC together, acGGA correlation with acPBEx (P-acGGA) is about 4 times more accurate for atoms than PBE is. However, B88 is so accurate throughout the table as well as asymptotically, that when combined with acGGA correlation (acGGA), its error is three times smaller again. Finally the addition of density-dependence to the correlation energy gradient in acGGA+ (B88 exchange and acGGA+ correlation) improves cancellation of error (relative to acGGA) up to the fourth row, and smooths out the fluctuations between even and odd rows.

We show the difference between density functional and QC correlation energies per electron for atoms with  $Z \leq 54$  in Fig. 6. PBE is, for much of the periodic table, roughly a constant shift off from QC reference data except for underperforming regions at the end of the second row and the middle of the fourth. The asymptotic correction of the PBE, acGGA, produces a nearly constant shift with respect to PBE for all  $Z$ , indicating that it has a nearly exact representation of the overall general trend of correlation energies with  $Z$  but is no more sensitive to the details of shell structure than is PBE. The  $\beta(r_s)$  correction included in acGGA+ is a small perturbation upon these results, but as one might expect, is a noticeable improvement in the second row. The LYP correlation functional has an error that in addition to the uncontrolled growth with  $Z$  noted earlier, has rather large fluctuations even for lower rows of the periodic table.

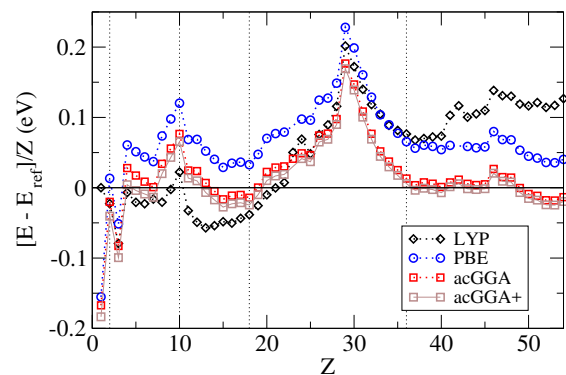


FIG. 6. Errors in correlation energy per electron as a function of atomic number. Closed shells indicated by vertical dotted lines.

In Fig. 7 we show errors in energy per electron for acGGA correlation, acPBEx, B88 exchange, and the combination of B88 with acGGA correlation. We note an eerie match of B88 exchange with acGGA correlation – both are exceptionally accurate for odd rows and exhibit a strong anticorrelation of error in even rows. The X and C errors are like mirror images, so that they largely cancel one another, just as in LDA, making XC much more accurate than X. The worst actors ( $Z = 10, 29, 30, 70$ ) are the same for both X and C. The cancellation of X and

| p   | $E_C$ |       |       |       |       |        | $E_{XC}$ |         |       |        |
|-----|-------|-------|-------|-------|-------|--------|----------|---------|-------|--------|
|     | acRPA | LDA   | LYP   | PBE   | acGGA | acGGA+ | PBE      | P-acGGA | acGGA | acGGA+ |
| 1   | N/A   | 0.765 | 0.011 | 0.084 | 0.094 | 0.112  | 0.216    | 0.032   | 0.039 | 0.037  |
| 2   | N/A   | 0.924 | 0.024 | 0.067 | 0.038 | 0.032  | 0.304    | 0.018   | 0.080 | 0.070  |
| 3   | N/A   | 1.032 | 0.047 | 0.045 | 0.014 | 0.018  | 0.297    | 0.104   | 0.023 | 0.013  |
| 4   | N/A   | 1.002 | 0.082 | 0.113 | 0.061 | 0.055  | 0.355    | 0.114   | 0.016 | 0.014  |
| 5   | 0.003 | 1.082 | 0.107 | 0.055 | 0.010 | 0.010  | 0.433    | 0.083   | 0.010 | 0.013  |
| 6   | 0.015 | 1.034 | 0.271 | 0.120 | 0.067 | 0.063  | 0.472    | 0.082   | 0.041 | 0.045  |
| All | N/A   | 1.020 | 0.146 | 0.092 | 0.047 | 0.044  | 0.401    | 0.084   | 0.031 | 0.031  |

TABLE I. Mean absolute error (eV) of energy components per electron, taken with respect to our reference data set, and averaged over each period ( $p$ ) of the periodic table. (The reference data set is given in Ref. 32, and consists of QC data for  $Z \leq 54$  and asymptotically corrected RPA (acRPA in Ref. 32) for  $p = 5$  and 6.) acRPA is RPA adjusted to match the asymptotic limit of quantum chemistry data, and used to fill in  $Z$  values in that data for  $p = 5$  and 6.

C errors likely is attributable to a cancellation between X and C holes, as the latter is affected by the screening characteristics of the former. (A classic example is the long range tail in the exchange hole in a uniform gas inducing a long range tail in correlation hole which cancels the effect. The effect is to decrease the magnitude of the LDA exchange energy and increase that of LDA correlation relative to the exact values for any non-metal or finite system.)

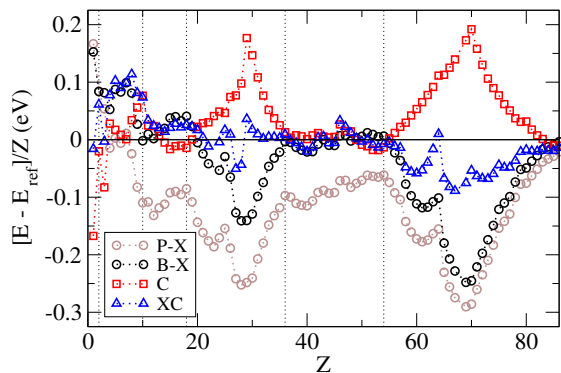


FIG. 7. Errors in XC components per electron as a function of  $Z$  for acGGAc (C), acPBEx (P-X), B88 exchange (B-X), and B88 exchange with acGGAc (XC). PBE errors are significantly larger (see Table I) and do not often cancel.

To begin to understand why the bad actors are who they are, note that asymptotic expansions fare worst when only the lowest level of a quantum system is occupied,<sup>80</sup> This happens here for each angular momentum,  $l$ . Consider  $n(\mathbf{r})$  as a sum of contributions with different angular shapes,  $n_l(\mathbf{r})$ . Whenever a given  $l$  value is first occupied, our errors should be largest. In the first octet, the lowest  $p$  orbitals are occupied (first singly, then doubly) across the row, leading to the largest error when full (Ne). The problem slowly goes away in the second octet, as each channel gains a  $3p$  occupant, but recurs when first filling the  $d$  orbitals, being worst for closed  $3d$ -shell atoms ( $Z = 29$ ) and Zn ( $Z = 30$ ), and again for the  $f$ -orbitals at Yb ( $Z = 70$ ). This is only a partial explanation of the phenomenon because the error recedes not with the first introduction of the second shell with the same angular momentum, but when the first is sucked

into the core with the introduction of additional valence shells. Possibly, the spatial isolation of such shells when in the valence amplifies their deviation from asymptotic behavior, but a more detailed explanation requires further research.

Finally, we note that acPBEx has qualitatively the same behavior as the B88 form, but never does quite as well as it in matching EXX energies. It noticeably approaches B88 as  $Z$  gets larger, naturally, because the two forms have the same  $B_x$  and must converge as  $Z \rightarrow \infty$ .

## B. Molecules

To test the effect of our asymptotic correction to the GGA for practical applications, we look at atomization energies of molecules – specifically those of the HEAT<sup>81</sup> and G2-1<sup>82</sup> data sets. Although we take an asymptotic analysis in the  $Z \rightarrow \infty$  limit, a good asymptotic expansion is useful for any system with  $Z^{-1} < 1$ . An improved asymptotic analysis should therefore provide a noticeable benefit for the thermochemistry of organic molecules – for which the typical values of  $Z^{-1}$  of many of the constituent elements are less than 0.2. We evaluate the approximate functionals on PBE orbitals as these systems are normal and the results should change little under self-consistency. All DFT calculations have been performed using a modified version of Turbomole 6.6.<sup>83</sup> Atom-centered Gaussian basis sets of valence quadruple-zeta plus polarization quality (def2-QZVP) are used for all atoms.<sup>84</sup> A fine density grid of quality 6 was employed for numerical integration.<sup>85</sup> The accuracy of different XC functionals was assessed for atomization energies using HEAT and G2-1 test sets. The results are compared with high-level coupled-cluster (CCSDTQ)<sup>81</sup> and CCSD(T)<sup>86</sup> calculations, and tabulated in the supplementary material for this article.

In Table II we show mean absolute errors, median errors, and maximum spread or difference between the most positive and most negative errors, across the HEAT and G2-1 test sets. The median error shows that PBE and BLYP<sup>59,78</sup> have a systematic tendency to overbind, although they are a great improvement on the LDA which

has a median overbinding of 38 kcal/mol. Both flavors of the acGGA reduce the overbinding of PBE. B88<sup>78</sup> exchange plus acGGA correlation (acGGA) has the best median value overall, cutting the overbinding error in PBE in half for the HEAT set, and even more dramatically for the G2-1. It has a somewhat larger maximum spread of errors compared to the LYP – it is less successful at improving the precision of PBE calculations than in correcting its median error. This leads to a somewhat larger MAE than that of BLYP. As with atoms, the inclusion of an  $r_s$ -dependent  $\beta$ , or acGGA+, improves only slightly upon the acGGA, indicating that the latter is already nearly optimal. The P-acGGA, using asymptotically correct acPBEx, has much less, but non-negligible, effect.

| Model      | HEAT  |       |       | G2-1 |       |       |
|------------|-------|-------|-------|------|-------|-------|
|            | MAE   | ME    | MS    | MAE  | ME    | MS    |
| BLYP       | 6.97  | 6.19  | 36.96 | 5.27 | 1.66  | 30.75 |
| PBE        | 11.51 | 11.51 | 50.02 | 8.52 | 5.33  | 44.29 |
| P-acGGA    | 10.10 | 9.01  | 45.16 | 7.25 | 3.96  | 40.72 |
| acGGA      | 7.64  | 5.25  | 43.52 | 5.88 | 1.41  | 38.95 |
| acGGA+     | 7.53  | 5.26  | 42.89 | 5.71 | 1.60  | 37.29 |
| B3LYP      | 2.90  | -0.19 | 26.44 | 2.78 | -0.69 | 21.35 |
| PBE0       | 3.40  | -1.64 | 29.22 | 3.45 | -1.42 | 18.17 |
| P-acGGA0   | 4.05  | -2.98 | 28.40 | 3.79 | -2.43 | 21.42 |
| acGGA0     | 6.08  | -5.54 | 28.76 | 5.46 | -5.15 | 24.40 |
| P-acGGAopt | 3.12  | -0.45 | 30.01 | 3.48 | -1.73 | 19.85 |
| acGGAopt   | 3.49  | -0.60 | 34.08 | 3.79 | -2.18 | 24.91 |
| acGGA+opt  | 3.37  | -0.65 | 33.45 | 3.59 | -1.94 | 23.61 |

TABLE II. Mean absolute error (MAE), median error (ME) and maximum spread (MS) of atomization energies of GGAs and hybrid functionals across 26 molecules of the HEAT data set<sup>81</sup> and 55 molecules of the G2-1 set,<sup>82</sup> in kcal/mol. Atoms have been excluded in both cases.

In Fig. 8, we show errors in atomization energies of the HEAT test set for several GGA and hybrid functionals, sorted by increasing size of PBE errors. The PBE errors strictly separate into three groups: molecules 0 – 9, each of which have a single non-hydrogen atom, 10 – 24, which have two, and molecule 25, carbon dioxide, which has three non-hydrogen atoms and the largest error. They group only crudely along the number of electrons in the molecule or other measures. The PBE is already very good for the first set, and the acGGA only slightly improves upon it. There is a definite improvement for P-acGGA when one moves to the two non-hydrogen atom set, and most improvement for CO<sub>2</sub>. The same pattern is followed by the acGGA and BLYP which closely match each other on a per-atom basis. For the G2-1 data set, the same trend occurs – P-acGGA is only a minimal change from PBE for molecules with only one non-hydrogen but a noticeable improvement of about 10 kcal/mol for two such atoms and even more for three. Conversely, the small improvement provided by the acGGA+ for low  $r_s$  shows up only for the H-rich molecules where acGGA is least effective, leading to the lower maximum spread shown in Table II. This pattern is consistent with our

hypothesis that the asymptotic correction of a functional is relevant for any  $Z > 1$ , as it has the most noticeable effect for molecules in which second row atoms and not hydrogen are the dominant players.

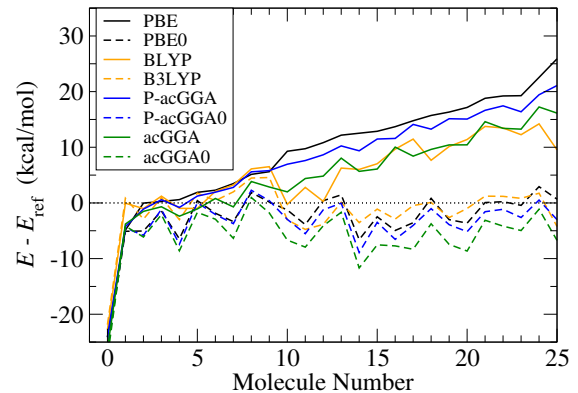


FIG. 8. Atomization energy errors across the HEAT data set, sorted via PBE errors. P-acGGA is acGGA correlation with asymptotically corrected PBE exchange, acGGA with B88 exchange. Hybrids P-acGGA0 and acGGA0 evaluated with 25% mixing of HF with semilocal exchange.

With the hybrids, the story is different. We calculate parameter-free “DFT0” hybrids, made by combining strictly 25% HF exchange with DFT exchange,<sup>87</sup> and compare to common hybrids PBE0<sup>87,88</sup> and B3LYP.<sup>89,90</sup> The empirically fit B3LYP is the best of this class, and no acGGA 25% hybrid improves upon PBE0. Fig. 9 shows that the asymptotic corrections we have made to the acGGA, either exchange or correlation, have little effect on the size of hybrid correction as long as a fixed 25% mixing is taken. The 25% hybrid correction in PBE0 is nearly optimal, with a small amount of underbinding in the median for both HEAT and G2-1. The underbinding correction of the acGGA that makes it the best overall GGA also makes it the worst 25% hybrid, as the median errors for each version are shifted down by almost exactly the same amount upon hybridization. As a result, MAE’s are reduced by much less than one might hope for with 25% mixing. However, one can reproduce or slightly improve PBE0 MAE for empirical acGGA hybrids, by mixing a smaller fraction of HF exchange (20% HF exchange with acPBEx exchange or 14% with B88). This is similar to hybrids of meta-GGAs, such as the TPSSh, the hybrid of the TPSS meta-GGA and exact exchange, which is optimized at 10% mixing.<sup>91</sup> The results (P-acGGAopt and acGGAopt) are then close to those of PBE0. Hybrids formed from the acGGA+ are optimized with the same amount of mixing as those formed from the acGGA and are again only a small improvement on the latter. In all, acGGA ought to be a better starting point than PBE, requiring smaller fractions of HF exchange to produce accuracies similar to PBE0.

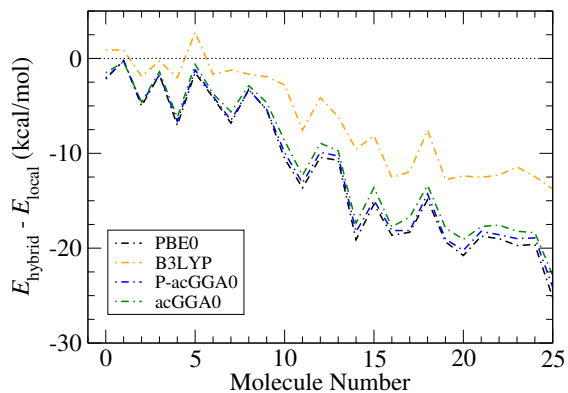


FIG. 9. Difference across the HEAT data set between the atomization energy evaluated with various hybrid functionals of Fig. 8 and the related semilocal functionals.

## V. IMPLICATIONS AND CONCLUSIONS

In this section, we discuss the implications of our effort to construct an asymptotically correct density functional.

### A. Relevance of the $Z \rightarrow \infty$ limit

The main implication of our work is the demonstration for the correlation energy, of the importance of  $\zeta$ -scaling; in particular, the importance of the  $Z \rightarrow \infty$  limit for all neutral atoms with  $Z > 1$ . We see that the asymptotic expansion for correlation derived in our previous work, implemented into an asymptotic functional for the  $r_s = 0$  limit of the correlation energy, by itself accounts for 80% or more of the beyond-LDA correlation for closed shell atoms down to Be. Integrating this limit with other constraints, most notably the low density, finite  $t$  limit of the PBE, generates a functional that is highly accurate for nearly all atoms. It seems to be the interplay of constraints, that necessarily become “entangled” with each other that does this; the form of the asymptotic limit of the GGA imposes specific conditions on the nature of the correlation cutoff function  $f_c$ , and thus propagates information on the  $r_s = 0$  limit to the functional at all  $r_s$ . The improvements are thus not limited to heavy atoms, but are significant even in the second row of the periodic table. Most notably, the asymptotic limit has an effect on the bonding characteristics of small- $Z$  molecules – atomization energies are noticeably improved over the PBE whenever there are bonds between two or more  $Z > 1$  atoms.

One question that our work does not quite resolve is why does PBE correlation parallel the beyond- $B_C$ , low- $Z$  behavior of QC so well? PBE correlation seems uncannily successful – satisfying constraints in limiting cases need not guarantee the level of accuracy of PBE (and therefore of the acGGA) for intermediate situations. As an illustration of this point, note the difference in performance of the Padé and B88 forms for acGGA exchange. Both meet

the same constraints in the limit of large  $Z$  and are reasonable parametrizations of the RSC exchange energy for moderate levels of inhomogeneity, but the B88 is clearly superior in recovering atomic exchange-correlation energies and molecular atomization energies. It could be argued that in each case (PBE correlation and B88 exchange) one uses the two best possible constraints for  $Z \sim 1$  and  $Z \rightarrow \infty$  systems, which then is sufficient to nail down the energies of most atoms. The Padé form for PBE exchange was designed, as much as possible, for universal applicability (here, ensuring the global Lieb-Oxford bound for any system) and not for optimal behavior for a specific class of systems.

### B. Functional development

We briefly consider the implications of our work for future functional development.

Despite our optimization of the basic form of the GGA for atomic energies, we expect that there is nearly as much room in functional space for tuning GGA correlation as there has been for exchange. The “internal enhancement factor”  $f_c$  used to modify the high density form of PBE is as open to variation as the enhancement factor  $F_x$  is for exchange. The two functions incorporate an intriguingly similar scaling form; and though not completely invariant under uniform scaling, the scaled variable  $y$  used in  $f_c$  is close to  $s$ , the invariant argument used in exchange. Each thus describes a transition between small- $s$  and large- $s$  limits. At the same time, the large- $r_s$  form for  $\beta(r_s)$  is open to improvement, as it is largely unknown.  $f_c$  and  $\beta$  may be manipulated together to come up with an infinite variety of forms that preserve asymptotic correctness and the correlation energies of atoms at finite  $Z$ , while meeting other conditions, perhaps on the potential.

Our work naturally also has consequences for higher rungs of functional development, as we have already discussed in regards to hybrids. The standard next step beyond the GGA in functional development is the meta-GGA which adds information obtained from the local Kohn-Sham kinetic energy,  $\tau^{\text{KS}}$ , in addition to the local density and gradient. A common approach to meta-GGA development is to parametrize corrections to the GGA in terms of an electron localization measure,<sup>2,17</sup>

$$\alpha = \frac{\tau^{\text{KS}} - \tau^{\text{W}}}{\tau^{\text{TF}}} \quad (38)$$

where  $\tau^{\text{KS}} = (1/2) \sum_i^{\text{Nocc}} |\nabla \phi_i|^2$ , and is calculated with occupied KS orbitals  $\phi_i$ ,  $\tau^{\text{W}} = |\nabla n|^2 / 8n$  is the von Weizsacker kinetic energy functional and  $\tau^{\text{TF}}$ , the TF energy density. This measure is closely related to the electron localization factor (ELF),<sup>92,93</sup> and like the ELF, distinguishes between three limit cases. The limit  $\alpha = 0$  indicates single orbital occupation, typified by covalent single bonds,  $\alpha = 1$  the highly-degenerate electron gas, and

thus metallic bonds, and  $\alpha \rightarrow \infty$ , regions of asymptotically low electron densities such as ionic bonds. Typically, a constraint-based meta-GGA tries to handle each case with a different exchange-correlation functional.<sup>2</sup>

Within the context of meta-GGAs, our work is immediately relevant to the high-density, high-degeneracy limit, or  $\alpha=1$  and  $r_s=0$ , the limit of  $\zeta \rightarrow \infty$  in Lieb-Simon scaling. In order to reproduce the correct  $B_C$  coefficient in the asymptotic expansion for correlation, the correlation functional should reduce to something like Eq. (30) in this limit. In addition, the beyond- $B_C$  asymptotic trend of Eq. (13) involves a transition from  $\alpha=1$  for  $Z \rightarrow \infty$  to  $\alpha=0$  as one reaches the He spin singlet. Matching the correlation energies of closed shell atoms for finite  $Z$  could be an appropriate norm for determining this transition, and this is used in the construction of the recent constraint-based SCAN meta-GGA functional. SCAN’s reliance upon non-asymptotically corrected PBE correlation implies an inaccurate value for  $B_C$ , but on a scale that is likely irrelevant to the resulting approximation.

The approach taken in our work may also be useful beyond its immediate scope – to analyze directly the standard ingredients of meta-GGAs. As we have noted earlier, Lieb-Simon scaling analysis has produced an estimate of the fourth-order gradient correction of exchange in atoms<sup>26</sup>; in addition it has been used to deduce the large- $Z$  limit of  $\alpha$  for atoms, and to show that it has relevance for physical values of  $Z$ .<sup>94</sup>

### C. Limits of the asymptotic correction

Perhaps the most interesting physical issue raised by our work is the separation of the periodic table into sections that are close to the asymptotic limit and others that are not. We note that this misfit is maximum for *closed-shell* atoms and not, as one might expect, for open-shell systems. The apparently relevant argument as one fills the 3d shell or 4f shell is the filling fraction of the shell, not other details such as non-spherical potentials. Open-shell structural effects are in comparison only responsible for low level “noise” in the overall trend. To account for the majority of the remaining exchange and correlation error in atoms, a next-order correction to the acGGA need, quite contrary to our initial expectations, only look at failure modes for spherical, unpolarized systems.

Significantly, the little data we have to characterize this trend shows no evidence that the problem would eventually go away for very large  $Z$ . Our functional is close to ideal for exactly one-half of the periodic table (odd rows) despite no consideration of any open-shell system, but still substantially in error for the other half (even). There is a possibility that there is a dependence of the asymptotic coefficients  $B_X$  and  $B_C$  with filling fraction for these bad rows, not obtainable from an extrapolation that considered atoms only from near the boundaries of each row. Such behavior is not unexpected in asymptotic

analysis, appearing for example, in the expansion of total energy of the Bohr (noninteracting) atom.<sup>32</sup> Careful asymptotic analysis of this trend for exchange, to which correlation seems to be a response, and careful consideration of functionals that could model this effect would both be very welcome.

### D. Conclusion

The central result of this paper is the construction of a density functional for correlation that satisfies the leading-order correction to LDA correlation in the large- $Z$  limit of neutral atoms as determined from the best QC data available. The functional is implemented as a modification to the PBE generalized gradient approximation, the simplest possible level of density functional at which this asymptotic correction can be obtained. The importance of this limit for all electronic structure is shown by its impact on the correlation energies for the entire periodic table and atomization energies for molecules of standard thermochemistry test sets. Together with an asymptotically correct exchange, this functional is close to the best parametrization of the energy of atoms across the periodic table that may be constructed at the GGA level. Our functional should thus serve as a starting point and a benchmark for constructing improved meta-GGA and hybrid functionals.

### SUPPLEMENTARY MATERIAL

See supplementary material for the specification of the acGGA functional and its potential, and for tables of atomic exchange and correlation energies and atomization energies for the HEAT and G-21 data sets.

### ACKNOWLEDGMENTS

This work was supported by NSF CHE-1464795. We thank John Perdew and Jianwei Sun for many useful discussions and Eberhard Engel for use of his atomic DFT code, OPMKS.

### Appendix A: Divergence of gradient expansion for correlation

The naive gradient expansion for correlation in the Lieb-Simon asymptotic limit is

$$E_C^{aGE} = \gamma \ln(r_s) + \eta + \beta(r_s)t^2. \quad (\text{A1})$$

where the first two terms give the high-density RPA limit of the LDA, Eq. (6). It is not shown in our plots. It is too large even for finite atoms, being over 100 mHa for Neon. Secondly, it diverges logarithmically for large  $Z$ .

This is a surprising result, as  $t^2(\mathbf{r})$  scales as a constant under  $\zeta$ -scaling. But it may be explained as follows:

While  $t^2(\mathbf{r})$  does scale as a constant under  $\zeta$ -scaling, that constant tends to infinity at the nucleus because the scaled density does too in the TF limit. Take the following convenient expressions<sup>30</sup> for the radial particle density and  $t^2$  as  $r \rightarrow 0$ :

$$4\pi r^2 n^{\text{TF}}(\mathbf{r}) dr \rightarrow Z x^{1/2} dx \quad (\text{A2})$$

and

$$t^2 \rightarrow \frac{a_2^2}{x^{3/2}} \quad (\text{A3})$$

where

$$x = Z^{1/3} r/a \quad (\text{A4})$$

and  $a = (1/2)(3\pi/4)^{2/3}$  and  $a_2 \sim 0.6124$ . The expression for the GEA contribution to the energy in this limit is

$$E_C^{\text{GEA}} = Z a_2^2 \int_0^\infty x'^{-1} dx' \sim \ln(x)|_0 \quad (\text{A5})$$

For a finite  $Z$  system the logarithmic divergence is cured by the transition to the nuclear cusp occurring around  $r = a_0/Z$  or  $x = a_0/aZ^{2/3}$ . The density no longer diverges as  $1/x^{3/2}$  but goes to some definite finite value. If we take the lower limit of the integral over the diverging Thomas-Fermi density to be  $a_0/Z$  this diverging term becomes:

$$E_C^{\text{GEA}} \rightarrow Z a_2^2 \ln(aZ^{2/3}/a_0), \quad (\text{A6})$$

or

$$E_C^{\text{GEA}} \rightarrow \frac{2a_2^2}{3} Z \ln Z. \quad (\text{A7})$$

Thus, the GE produces a finite contribution of order  $Z \ln Z$  to the asymptotic expansion of the energy of neutral atoms. This contribution is spurious, as the work of Kunz and Rueedi<sup>41</sup> already implied that the coefficient of this term is exactly given by LDA correlation.

## Appendix B: Derivation of asymptotically corrected $H_C$

To find an analytic value of  $\tilde{c}$  in Eq. (31), we derive RSC in the large- $Z$  limit. Appendix C of Ref. 64 gives formulas for RSC as  $r_s \rightarrow 0$ . Both the LDA and GEA correlation holes are given in terms of a short-ranged contribution (on the scale of  $1/k_F$ ) and a long-ranged contribution (on the scale of  $1/k_s$ ). As  $r_s \rightarrow 0$ , the short-ranged pieces do not contribute. The long-ranged radial LDAc hole tends to a constant as  $v = k_s u \rightarrow 0$ , so the energy integral has a  $1/v$  term, the cutoff of which produces the  $\ln r_s$  contribution to the correlation energy in Eq. 6. As  $t$  becomes large, the cut-off  $v_C$  is very small, producing the logarithmic divergence with  $t$ .

Although PBE removes the logarithmic divergence, we have seen it clearly differs from the RSC in the next order. Define

$$C = \lim_{t \rightarrow \infty} [H_C^{\text{GGA}}(0, t) - 2\gamma \ln t], \quad (\text{B1})$$

to find  $C^{\text{PBE}} = \gamma \ln(\beta/\gamma) = 0.0237$ . For the real-space construction, define

$$\gamma = \lim_{\epsilon \rightarrow 0} \int_\epsilon^\infty dv \frac{f_1(v) - 4\gamma}{2v}, \quad (\text{B2})$$

where  $v = k_s u$  and  $f_1(v)$  is the dimensionless radial  $n_C^{\text{LDA}}(u)$  in RPA. Then

$$C^{\text{RSC}} = \gamma \left[ 3 - 2 \ln \left( 3\pi \sqrt{6\gamma} \right) \right] + \gamma, \quad (\text{B3})$$

which is about -0.0044 with the models of Ref. 64. Then take  $\gamma \ln \tilde{c}^{\text{RSC}} = C^{\text{PBE}} - C^{\text{RSC}}$ , to yield  $\tilde{c} = 2.4683$ .

- <sup>1</sup>J. P. Perdew and K. Schmidt, in *Density Functional Theory and Its Applications to Materials*, edited by V. E. V. Doren, K. V. Alsenoy, and P. Geerlings (American Institute of Physics, Melville, NY, 2001).
- <sup>2</sup>J. Sun, A. Ruzsinszky, and J. P. Perdew, *Phys. Rev. Lett.* **115**, 036402 (2015).
- <sup>3</sup>J. P. Perdew, K. Burke, and M. Ernzerhof, *Phys. Rev. Lett.* **77**, 3865 (1996), *ibid.* **78**, 1396(E) (1997).
- <sup>4</sup>A. Pribram-Jones, D. A. Gross, and K. Burke, *Annual Review of Physical Chemistry* (2015).
- <sup>5</sup>J. Perdew, *Phys. Rev. Lett.* **55**, 1665 (1985).
- <sup>6</sup>K. Burke, J. P. Perdew, and Y. Wang, "Derivation of a generalized gradient approximation: The pw91 density functional," in *Electronic Density Functional Theory: Recent Progress and New Directions*, edited by J. F. Dobson, G. Vignale, and M. P. Das (Plenum, NY, 1997) p. 81.
- <sup>7</sup>A. Becke, *J. Chem. Phys.* **109**, 2092 (1998), <http://dx.doi.org/10.1063/1.476722>.
- <sup>8</sup>E. I. Proynov and D. R. Salahub, *J. Chem. Phys.* **49**, 7874 (1994).
- <sup>9</sup>M. Filatov and W. Thiel, *Phys. Rev. A* **57**, 189 (1998).
- <sup>10</sup>J. P. Perdew and L. A. Constantin, *Phys. Rev. B* **75**, 155109 (2007).
- <sup>11</sup>A. C. Cancio, C. E. Wagner, and S. A. Wood, *International Journal of Quantum Chemistry* **112**, 3796 (2012).
- <sup>12</sup>D. Mejia-Rodriguez and S. B. Trickey, *Phys. Rev. A* **96**, 052512 (2017).
- <sup>13</sup>J. P. Perdew, S. Kurth, A. c. v. Zupan, and P. Blaha, *Phys. Rev. Lett.* **82**, 2544 (1999).
- <sup>14</sup>J. Tao, J. P. Perdew, V. N. Staroverov, and G. E. Scuseria, *Phys. Rev. Lett.* **91**, 146401 (2003).
- <sup>15</sup>J. P. Perdew, A. Ruzsinszky, G. I. Csonka, L. A. Constantin, and J. Sun, *Phys. Rev. Lett.* **103**, 026403 (2009).
- <sup>16</sup>J. P. Perdew, A. Ruzsinszky, G. I. Csonka, L. A. Constantin, and J. Sun, *Phys. Rev. Lett.* **106**, 179902 (2011).
- <sup>17</sup>J. Sun, R. Haunschuld, B. Xiao, I. W. Bulik, G. E. Scuseria, and J. P. Perdew, *The Journal of Chemical Physics* **138** (2013).
- <sup>18</sup>J. Sun, B. Xiao, Y. Fang, R. Haunschuld, P. Hao, A. Ruzsinszky, G. I. Csonka, G. E. Scuseria, and J. P. Perdew, *Phys. Rev. Lett.* **111**, 106401 (2013).
- <sup>19</sup>J. P. Perdew, in *Electronic Structure of Solids '91*, edited by P. Ziesche and H. Eschrig (Akademie Verlag, Berlin, 1991).
- <sup>20</sup>J. P. Perdew, A. Ruzsinszky, G. I. Csonka, O. A. Vydrov, G. E. Scuseria, L. A. Constantin, X. Zhou, and K. Burke, *Phys. Rev. Lett.* **100**, 136406 (2008).
- <sup>21</sup>Y. Zhao and D. G. Truhlar, *J. Chem. Phys.* **128**, 184109 (2008).
- <sup>22</sup>A. Vela, V. Medel, and S. B. Trickey, *J. Chem. Phys.* **130**, 244103 (2009).



- <sup>23</sup>A. Ruzsinszky, G. I. Csonka, and G. E. Scuseria, *J. Chem. Theory Comput.* **5**, 763 (2009).
- <sup>24</sup>L. A. Constantin, E. Fabiano, S. Laricchia, and F. Della Sala, *Phys. Rev. Lett.* **106**, 186406 (2011).
- <sup>25</sup>J. M. del Campo, J. L. Gázquez, S. B. Trickey, and A. Vela, *J. Chem. Phys.* **136**, 104108 (2012).
- <sup>26</sup>L. A. Constantin, A. Terentjevs, F. Della Sala, P. Cortona, and E. Fabiano, *Phys. Rev. B* **93**, 045126 (2016).
- <sup>27</sup>J. C. Pacheco-Kato, J. M. del Campo, J. L. Gázquez, S. Trickey, and A. Vela, *Chemical Physics Letters* **651**, 268 (2016).
- <sup>28</sup>J. P. Perdew, L. A. Constantin, E. Sagvolden, and K. Burke, *Phys. Rev. Lett.* **97**, 223002 (2006).
- <sup>29</sup>P. Elliott, D. Lee, A. Cangi, and K. Burke, *Phys. Rev. Lett.* **100**, 256406 (2008).
- <sup>30</sup>D. Lee, L. A. Constantin, J. P. Perdew, and K. Burke, *J. Chem. Phys.* **130**, 034107 (2009).
- <sup>31</sup>P. Elliott and K. Burke, *Can. J. Chem.* **87**, 1485 (2009).
- <sup>32</sup>K. Burke, A. Cancio, T. Gould, and S. Pittalis, *J. Chem. Phys.* **145**, 054112 (2016).
- <sup>33</sup>E. Lieb and B. Simon, *Phys. Rev. Lett.* **31**, 681 (1973).
- <sup>34</sup>E. H. Lieb and B. Simon, *Advances in Mathematics* **23**, 22 (1977).
- <sup>35</sup>E. H. Lieb, *Rev. Mod. Phys.* **53**, 603 (1981).
- <sup>36</sup>J. Scott, *Philos. Mag.* **43**, 859 (1952).
- <sup>37</sup>J. Schwinger, *Phys. Rev. A* **22**, 1827 (1980).
- <sup>38</sup>J. Schwinger, *Phys. Rev. A* **24**, 2353 (1981).
- <sup>39</sup>B.-G. Englert and J. Schwinger, *Phys. Rev. A* **32**, 26 (1985).
- <sup>40</sup>B.-G. Englert, *Semiclassical theory of atoms*, Lecture Notes in Physics, Vol. 300 (Springer Verlag, Berlin, 1988).
- <sup>41</sup>H. Kunz and R. Ruedi, *Phys. Rev. A* **81**, 032122 (2010).
- <sup>42</sup>R. F. Ribeiro, D. Lee, A. Cangi, P. Elliott, and K. Burke, *Phys. Rev. Lett.* **114**, 050401 (2015).
- <sup>43</sup>R. Ribeiro and K. Burke, *Phys. Rev. B* **95**, 115115 (2017).
- <sup>44</sup>S. P. McCarthy and A. J. Thakkar, *J. Chem. Phys.* **134**, 044102 (2011).
- <sup>45</sup>S. P. McCarthy and A. J. Thakkar, *J. Chem. Phys.* **136**, 054107 (2012).
- <sup>46</sup>D. C. Langreth and M. J. Mehl, *Phys. Rev. B* **28**, 1809 (1983).
- <sup>47</sup>J. Perdew, *Phys. Rev. B* **33**, 8822 (1986).
- <sup>48</sup>K. Burke, A. Cancio, T. Gould, and S. Pittalis, *submitted and arXiv:1409.4834v1* (2014).
- <sup>49</sup>S. Fournais, M. Lewin, and J. P. Solovej, *ArXiv e-prints* (2015), [arXiv:1510.01124 \[math-ph\]](https://arxiv.org/abs/1510.01124).
- <sup>50</sup>The energy as a function of the smooth variable  $\zeta$  has complications such as derivative discontinuities at integer  $Z$ . These corrections to  $E_{TF}(\zeta)$  become vanishingly small in the Lieb-Simon limit. Corrections to  $E_{TF}$  at the GGA level yield continuous curves that are more accurate at integer  $Z$ , without addressing these discontinuities.
- <sup>51</sup>The true gradient expansion only yields the leading corrections in cases without classical turning points, such as slowly varying gases. The presence of turning points typically alters the coefficients in the expansion without changing the functional form.<sup>28</sup> Hence the need for a *generalized* gradient approximation for the XC problem.
- <sup>52</sup>L. H. Thomas, *Math. Proc. Camb. Phil. Soc.* **23**, 542 (1927).
- <sup>53</sup>E. Fermi, *Zeitschrift für Physik A Hadrons and Nuclei* **48**, 73 (1928).
- <sup>54</sup>M. Gell-Mann and K. Brueckner, *Phys. Rev.* **106**, 364 (1957).
- <sup>55</sup>J. P. Perdew and Y. Wang, *Phys. Rev. B* **45**, 13244 (1992).
- <sup>56</sup>W. Kohn and L. J. Sham, *Phys. Rev.* **140**, A1133 (1965).
- <sup>57</sup>L. Kleinman and S. Lee, *Phys. Rev. B* **37**, 4634 (1988).
- <sup>58</sup>S. J. Chakravorty, S. R. Gwaltney, E. R. Davidson, F. A. Parpia, and C. F. Fischer, *Phys. Rev. A* **47**, 3649 (1993).
- <sup>59</sup>C. Lee, W. Yang, and R. G. Parr, *Phys. Rev. B* **37**, 785 (1988).
- <sup>60</sup>This disagrees slightly with our previous result,<sup>32</sup> reflecting a small error in weighting points in the latter.
- <sup>61</sup>W. H. Miller, *J. Chem. Phys.* **48**, 1651 (1968).
- <sup>62</sup>D. C. Langreth and J. P. Perdew, *Phys. Rev. B* **21**, 5469 (1980).
- <sup>63</sup>J. P. Perdew, K. Burke, and Y. Wang, *Phys. Rev. B* **54**, 16533 (1996), *ibid.* **57**, 14999(E) (1998).
- <sup>64</sup>K. Burke, J. P. Perdew, and Y. Wang, “Derivation of a generalized gradient approximation: The pw91 density functional,” in *Electronic Density Functional Theory: Recent Progress and New Directions*, edited by J. F. Dobson, G. Vignale, and M. P. Das (Plenum, NY, 1997) p. 81.
- <sup>65</sup>J. Harris and R. Jones, *J. Phys. F* **4**, 1170 (1974).
- <sup>66</sup>D. Langreth and J. Perdew, *Solid State Commun.* **17**, 1425 (1975).
- <sup>67</sup>O. Gunnarsson and B. Lundqvist, *Phys. Rev. B* **13**, 4274 (1976).
- <sup>68</sup>J. P. Perdew and Y. Wang, *Phys. Rev. B* **46**, 12947 (1992).
- <sup>69</sup>R. Jones and O. Gunnarsson, *Rev. Mod. Phys.* **61**, 689 (1989).
- <sup>70</sup>K. Burke, J. P. Perdew, and M. Ernzerhof, *The Journal of Chemical Physics* **109**, 3760 (1998).
- <sup>71</sup>A. C. Cancio and C. Y. Fong, *Phys. Rev. A* **85**, 042515 (2012).
- <sup>72</sup>M. Levy, *Int. J. Quantum Chem.* **S23**, 617 (1989).
- <sup>73</sup>M. Levy, *Phys. Rev. A* **43**, 4637 (1991).
- <sup>74</sup>C. Hu and D. Langreth, *Phys. Scr.* **32**, 391 (1985).
- <sup>75</sup>M. Rasolt and D. Geldart, *Phys. Rev. B* **34**, 1325 (1986).
- <sup>76</sup>D. Geldart and M. Rasolt, *Phys. Rev. B* **13**, 1477 (1976).
- <sup>77</sup>We choose to alter  $\tilde{c}_{AC}$  rather than  $\eta$  because the GE hole in the  $r_s = 0$  limit is well-known<sup>46</sup>, leaving the crude cutoff method employed as the major source of error in the RSC. Large- $t$  features of the RSC GGA are thus those most likely to be in error.
- <sup>78</sup>A. D. Becke, *Phys. Rev. A* **38**, 3098 (1988).
- <sup>79</sup>E. Engel and R. M. Dreizler, *Journal of Computational Chemistry* **20**, 31 (1999).
- <sup>80</sup>A. Cangi, D. Lee, P. Elliott, and K. Burke, *Phys. Rev. B* **81**, 235128 (2010).
- <sup>81</sup>A. Tajti, P. G. Szalay, A. G. Császár, M. Kállay, J. Gauss, E. F. Valeev, B. A. Flowers, J. Vázquez, and J. F. Stanton, *The Journal of Chemical Physics* **121**, 11599 (2004).
- <sup>82</sup>L. A. Curtiss, K. Raghavachari, P. C. Redfern, and J. A. Pople, *J. Chem. Phys.* **106**, 1067 (1997).
- <sup>83</sup>F. Furche, R. Ahlrichs, C. Hättig, W. Klopper, M. Sierka, and F. Weigend, *WIREs Comput. Mol. Sci.* **4**, 91 (2014).
- <sup>84</sup>F. Weigend, F. Furche, and R. Ahlrichs, *J. Chem. Phys.* **119**, 12753 (2003).
- <sup>85</sup>O. Treutler and R. Ahlrichs, *J. Chem. Phys.* **102**, 346 (1995).
- <sup>86</sup>D. Feller and K. A. Peterson, *J. Chem. Phys.* **110**, 8384 (1999).
- <sup>87</sup>J. P. Perdew, M. Ernzerhof, and K. Burke, *The Journal of Chemical Physics* **105**, 9982 (1996).
- <sup>88</sup>K. Burke, M. Ernzerhof, and J. P. Perdew, *Chemical Physics Letters* **265**, 115 (1997).
- <sup>89</sup>A. D. Becke, *The Journal of Chemical Physics* **98**, 5648 (1993).
- <sup>90</sup>P. J. Stephens, F. J. Devlin, C. F. Chabalowski, and M. J. Frisch, *J. Phys. Chem.* **98**, 11623 (1994).
- <sup>91</sup>V. N. Staroverov, G. E. Scuseria, J. Tao, and J. P. Perdew, *J. Chem. Phys.* **119**, 12129 (2003).
- <sup>92</sup>A. D. Becke and K. E. Edgecombe, *J. Chem. Phys.* **92**, 5397 (1990).
- <sup>93</sup>B. Silvi and A. Savin, *Nature* **371**, 683 (1994).
- <sup>94</sup>A. C. Cancio and J. J. Redd, *Molecular Physics* **115**, 618 (2017).